Progress in CTEQ-TEA (Tung et al.) PDF Analysis

Sayipjamal Dulat
Xinjiang University University
In collaboration with
CTEQ-TEA Group

April 4, 2016

QCD Study Group

CTEQ-TEA group

- CTEQ – Tung et al. (TEA)

in memory of Prof. Wu-Ki Tung,
who established CTEQ Collaboration in early 90's

- Current members:

Sayipjamal Dulat (Xinjiang Univ.),
Tie-Jiun Hou, Pavel Nadolsky (Southern Methodist Univ.),
Jun Gao (Argonne Nat. Lab.),
Marco Guzzi (Univ. of Manchester),
Joey Huston, Jon Pumplin, Dan Stump, Carl Schmidt,
and C.- P.Yuan (Michigan State Univ.)

Outline

- Parton Distribution Functions(PDFs)
- Overview of CT14 PDF results

  -- Effect from LHC Run 1 (ATLAS, CMS, LHCb) and new Tevatron D0 Data to CT14 PDFs

  -- Impact to Higgs and Top physics at LHC Run 2
- Summary

Parton Distribution Functions

Needed for making theoretical calculations to compare with experimental data

Hadron Collider Physics

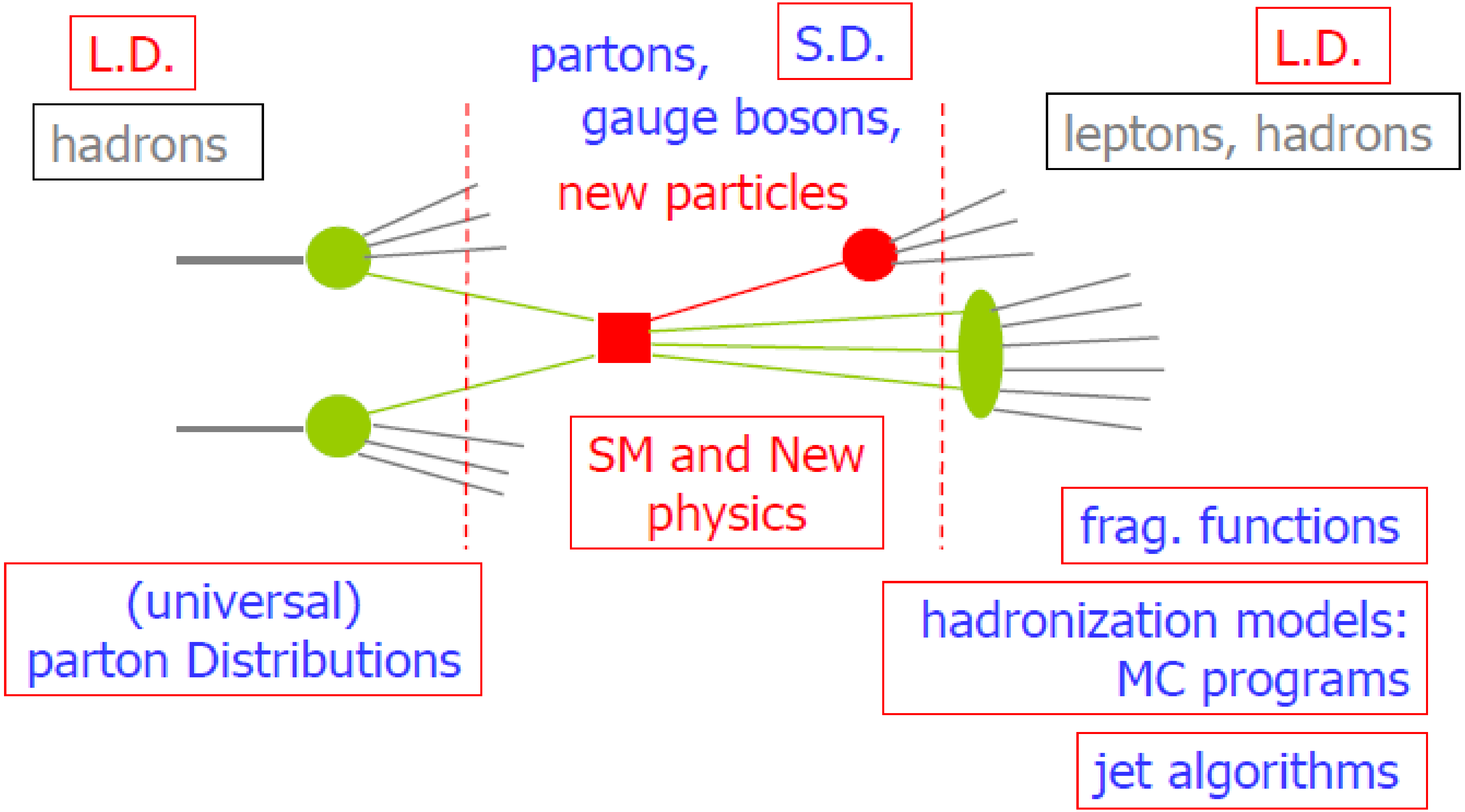

PDF groups

There are quite a number of groups performing fits in order to obtain parton distributionfunctions

- *ABM* by S. Alekhin, J. Bluemlein, S. Moch
- *CTEQ-TEA (CT* Collaboration
- *GRV/GJR*, from M. Glück, P. Jimenez-Delgado, E. Reya, and A. Vogt
- *HERA* PDFs, by H1 and ZEUS collaborations from the Deutsches Elektronen-Synchrotron center (DESY) in Germany
- *MRST/MSTW/MMHT*, from A. D. Martin, R. G. Roberts, W. J. Stirling, R. S. Thorne, and G. Watt
- *NNPDF* Collaboration

How are PDFs used?

CTEQ

Hard scattering cross sections

$$d\sigma^{h_1 h_2 \to cd} = \int_0^1 dx_1 \int_0^1 dx_2 \sum_{a,b} f_{a/h_1}(x_1, \mu_F^2) f_{b/h_2}(x_2, \mu_F^2) d\hat{\sigma}^{ab\to cd}(Q^2, \mu_F^2)$$

- $f_{a/hi}(x_i)$: parton distribution function: probability of finding a parton of type a with momentum fraction x_i in the hadron h_i
  - process-independent but not calculable in perturbation theory
  - needs to be determined from data
  - contains all unresolved emission below factorization scale μ_F
- $\sigma^{ab\to cd}$: parton-level hard scattering cross section
  - calculable in perturbative QCD as series expansion in α_s
  - contains only hard emissions above factorization scale μ_F

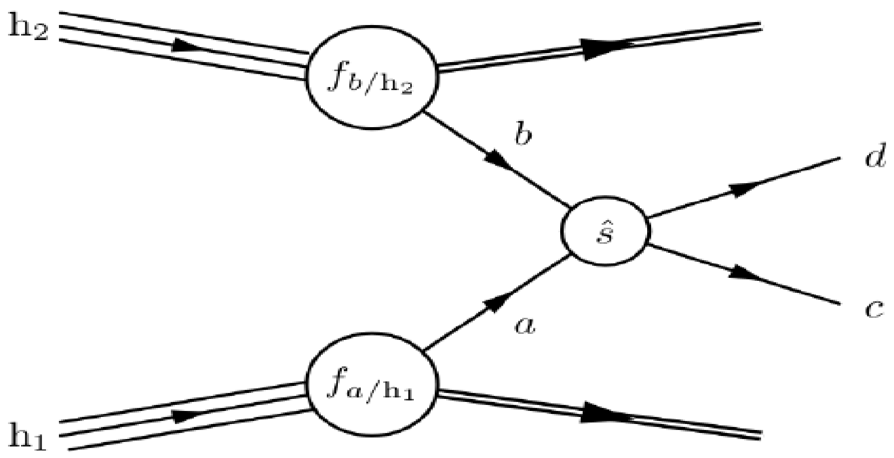

How are PDFs Measured?

- PDFs are measured by a global QCD analysis: simultaneously fitting a wide range of data from different experiments at $Q \geq Q0$.

The PDFs are a set of 11 functions,

$f_i(x,Q^2)$ where $\begin{cases} 0 \leq x \leq 1 & \text{longitudinal momentum fraction} \\ Q >\sim 2\ GeV & \text{momentum scale} \end{cases}$

$i = 0, \pm 1, \pm 2, \pm 3, \pm 4, \pm 5$ parton index

$f_0 = g(x,Q^2)$ the gluon PDF

$f_1 = u(x,Q^2)$ the up-quark PDF

$f_{-1} = \bar{u}(x,Q^2)$ the up-antiquark PDF

$f_2 = d$ and $f_{-2} = \bar{d}$

$f_3 = s$ and $f_{-3} = \bar{s}$

PDFs are universal –depend on the type of the hadron （p）and partons (q, qbar, g)

Global Fits

The problem: from data construct PDFs and their uncertainties.

1. Input from Experiment: select experimental data sets.
2. Input from theory: select hard scattering cross sections.
3. Asumptions: parametrize x-dependence of each flavor at small $Q_0 = 1.3GeV$.
4. Compute PDFs $f_a(x, Q)$ at $Q > Q_0$ by DGLAP evolution equation:

$$\mu \frac{df_{i/p}(x,\mu)}{d\mu} = \sum_{j=g,u,\bar{u},d\bar{d},\ldots} \int_x^1 \frac{dy}{y} P_{i/j}\left(\frac{x}{y}, \alpha_s(\mu)\right) f_{j/p}(y,\mu)$$

where $P_{i/j}$ are spilliting functions that describe the probability of a given parton splitting into two others ($j \to ik$);

$$P_{i/j}(x, \alpha_s) = \alpha_s P^{(1)}_{i/j} + \alpha_s^2 P^{(2)}_{i/j} + \alpha_s^3 P^{(3)}_{i/j} + \cdots$$

5. Construct

$$\chi^2_{global} = \sum_{e=1}^{N_{exp}} W_e \chi^2_e$$

$W_e > 0$ are weights applied to emphasize or de-emphasize contributions from individual experiments (default:$W_e = 1$).
There are N_{exp} experiments, e labels an experimental data set.
6. Minimize χ^2_{global} to find "Best Fit" PDFs.
7. Use the χ^2_{global} in neighborhood of the minimum to define PDF uncertainties.
Basic idea is to construct $2 \times d$ "alternative fits" near enough to $\{a_{01}, a_{02}, a_{03}, \cdots, a_{0d}\}$ to be good fits.

The χ^2 for one experiment is

$$\chi_e^2(\{a\},r) = \sum_{\nu=1}^{M_e} \frac{\left[D_\nu - \sum_{k=1}^{R_e} r_k \beta_{k\nu} - T_\nu(\{a\})\right]^2}{\sigma_\nu^2} + \sum_{k=1}^{R_e} r_k^2.$$

D_ν and $T_\nu(\{a\})$ are data and theory values at each point.

$\sigma_\nu = \sqrt{\sigma_{stat}^2 + \sigma_{syst}^2}$ is the total error.

M_e are data points in a particular set of data.

$\beta_{k\nu}$ are correlated systematic errors for each of the data points.

$\{r_k\}$ is a set of shift parameters, which is associated with the systematic errors.

$\sum_{k=1}^{R_e} r_k \beta_{k\nu}$ are correlated sytematic shifts applied to data points D_ν

$\sum_{k=1}^{R_e} r_k^2$ is a quadratic penalty term for non-zero values of the shifts r_k .

There are a few details to address

- Order of perturbation theory (LO, NLO, NNLO, . . .)
- Scheme dependence (MSbar, . . .)
- Choices for scales in the hard scattering processes
- Treatment of heavy quarks
- Effects due to choosing or deleting a given data set
- Choice of kinematic cuts
- Treatment of experimental errors
- Error estimates on the PDFs

Requirements for PDF parametrization

CTEQ

A. A valid set of $f_{a/p}(x,Q)$ must satisfy QCD sum rules

Valence sum rule

$$\int_0^1 [u(x,Q) - \bar{u}(x,Q)]\, dx = 2 \qquad \int_0^1 [d(x,Q) - \bar{d}(x,Q)]\, dx = 1$$

$$\int_0^1 [s(x,Q) - \bar{s}(x,Q)]\, dx = 0$$

With similar relations for c and b quarks

A proton has net quantum numbers of 2 u quarks + 1 d quark

Momentum sum rule

$$[\text{proton}] \equiv \sum_{a=g,q,\bar{q}} \int_0^1 x\, f_{a/p}(x,Q)\, dx = 1$$

momenta of all partons must add up to the proton's momentum

Through this rule, normalization of $g(x,Q)$ is tied to the first moments of quark PDFs

Requirements for PDF parametrization

B. A valid PDF set must **not** produce unphysical predictions for observable quantities

Example

- Any concievable hadronic cross section σ must be non-negative: $\sigma \geq 0$
  - this is typically realized by requiring $f_{a/p}(x, Q) > 0$
- Any cross section asymmetry A must lie in the range $-1 \leq A \leq 1$
  - this constrains the range of allowed PDF pararametrizations

C. PDF parametrizations for $f_{a/p}(x, Q)$ must be "flexible just enough" to reach agreement with the data, without reproducing random fluctuations

PDF Uncertainties

- There are three methods to calculate PDF uncertainties so far:

1. The Hessian Error Matrix Method.

Uncertainties of Predictions from Parton Distribution Functions II: The Hessian Method, J. Pumplin et al., Phys. Rev. D65:014013, 2002

2. The Lagrange Multiplier Method

Uncertainties of Predictions from Parton Distribution Functions I: The Lagrange Multiplier Method,
D. Stump et al., Phys. Rev D65:014012,2002

3. MonteCarlo Replica Method

Hessian Method

- The Hessian matrix is the matrix of second derivatives of χ^2 at the minimum

$$H_{ij} = \frac{1}{2}\left(\frac{\partial^2\chi^2}{\partial y_i\,\partial y_j}\right)_0$$

$y_i = a_i - a_i^0$ as the displacement of parameter a_i from its value a_i^0

To estimate the error on some observable X(a), one uses the "Master Formula"

Uncertainty for an observable X due to PDF is given by

$$\Delta X = \left|\nabla X\right| = \frac{1}{2}\sqrt{\sum_{i=1}^{N}\left(X_i^{(+)} - X_i^{(-)}\right)^2}$$

where $X_i^{(+)}$ and $X_i^{(-)}$ are the values of X computed from the two sets of PDFs along the ($\pm$) direction of the i-th eigenvector.

Analysis of correlation due to PDFs

CTEQ

Correlation cosine for observables X and Y:

$$\cos\varphi = \frac{\nabla X \bullet \nabla Y}{\Delta X \Delta Y} = \frac{1}{4\Delta X \Delta Y}\sum_{i=1}^{N}(X_i^{(+)} - X_i^{(-)})(Y_i^{(+)} - Y_i^{(-)})$$

Uncertainty for an observable X due to PDF is given by

$$\Delta X = \left|\nabla X\right| = \frac{1}{2}\sqrt{\sum_{i=1}^{N}(X_i^{(+)} - X_i^{(-)})^2}$$

where $X_i^{(+)}$ and $X_i^{(-)}$ are the values of X computed from the two sets of PDFs along the $(\pm)$ direction of the i-th eigenvector.

The tolerance arror ellipse is introduced to study correlation between two observables.

C T E Q

Correlation angle φ

Determines the parametric form of the $X-Y$ correlation ellipse

$$
\begin{aligned}
X &= X_0 + \Delta X \cos\theta \\
Y &= Y_0 + \Delta Y \cos(\theta + \varphi)
\end{aligned}
$$

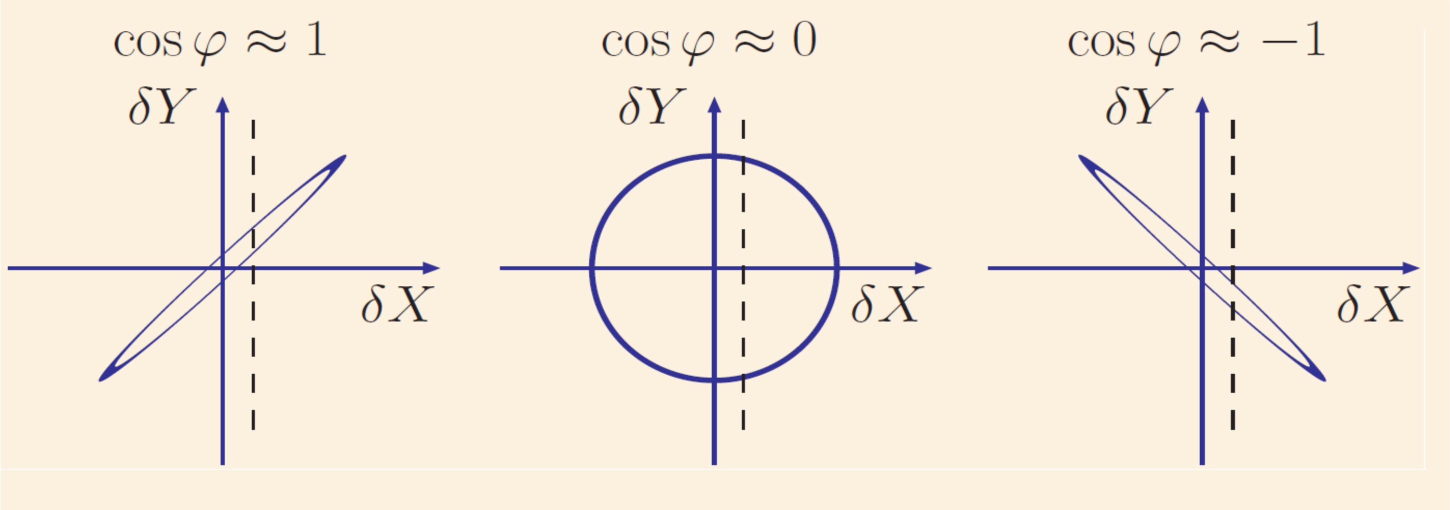

X_0, Y_0: best-fit values

ΔX, ΔY: PDF errors

$\delta X \equiv X - X_0$ and $\delta Y \equiv Y - Y_0$

$\cos\varphi \approx \pm 1$: Measurement of X imposes tight constraints on Y

$\cos\varphi \approx 0$: Measurement of X imposes loose constraints on Y

Types of Correlations

X and Y can be

- two PDFs $f_1(x_1, Q_1)$ and $f_2(x_2, Q_2)$ (plotted as $\cos\varphi$ vs x_1 & x_2)
- a physical cross section σ and PDF $f(x, Q)$ (plotted as $\cos\varphi$ vs x)
- two cross sections σ_1 and σ_2

Lagrange Multiplier Method

Consider a particular physical quantity, say $X(\{a_i\})$, which is a function of PDFs.

$$F(\lambda, \{a_i\}) = \chi^2(\{a_i\}) + \lambda(X(\{a_i\}) - X(\{a_i^{(0)}\}))$$

By minimizing this function with various fixed λ value, say $\lambda_1, \ldots\lambda_j\ldots, \lambda_n$, we will obtain d parameter sets $\{a_i(\lambda_j)\}$ and corresponding $X(\{a_i(\lambda_j)\})$ and $\chi^2(\{a_i(\lambda_j)\})$. With suitable choice of $\Delta\chi^2$, we obtain the uncertainty of the physical quantity $X(\{a_i\})$.

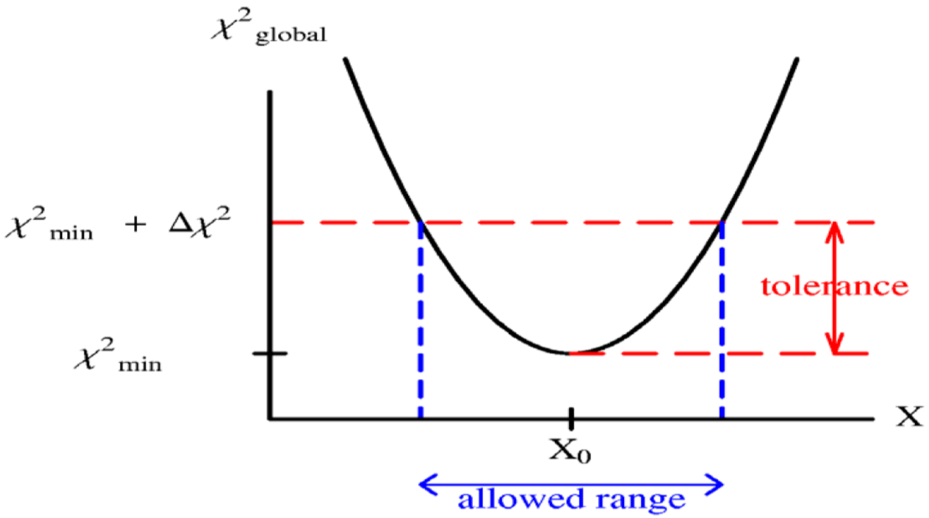

X : any variable that depends on PDF's
X_0 : the prediction in the standard set
$\chi^2(X)$: curve of constrained fits

For the specified tolerance ($\Delta\chi^2 = T^2$) there is a corresponding range of uncertainty, $\pm\Delta X$.

Overview of CT14 PDFs

- CT10 includes only pre-LHC data
- CT14 is the first CT analysis including LHC Run 1 data
- CT14 also includes the new Tevatron D0 Run 2 data on W-electron charge asymmetry
- CT14 uses a more flexible parametrization in the non-perturbative PDFs.
- Here, I will only show the CT14 results at NNLO. We have also published its results at NLO and LO.

arXiv:1506.07443, PRD 93, 033006(2016)

Experimental Data for CT14

- Based on CT10 data sets, but updated with new HERA F_L and F_2^c , and drop Tevatron Run 1 CDF and D0 inclusive jet data

- Included some LHC Run 1 data at 7 TeV:
  ATLAS and LHCb W/Z production,
  ATLAS, CMS and LHCb W-lepton charge asymmetry,
  ATLAS and CMS inclusive jet data

- Replaced the old D0 data (0.75 1/fb) by the new D0 (9.7 1/fb) W-electron rapidity asymmetry data.
- In order to reduce the PDF uncertainty, only those physical quantities which is not relative to hardronization are considered, such as inclusive DIS data, Drell-Yan data, W/Z production, and inclusive jet data.

LHC Run 1 Data matters

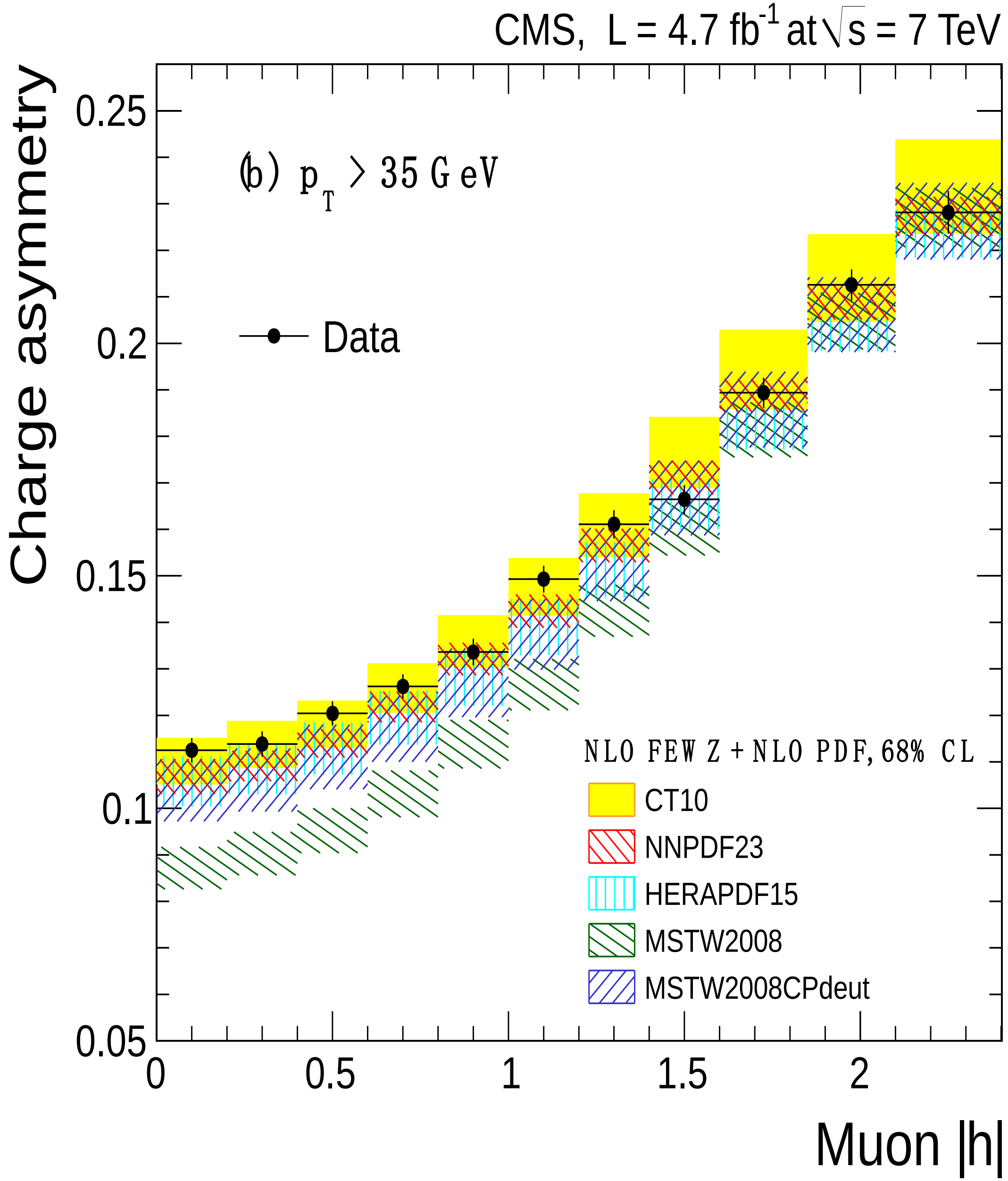

- Data is already more precise than CT10, NNPDF2.3 and MSTW2008 PDF uncertainties.
- Will help to determine u,d,ubar and dbar PDFs.
- Most useful for determining d/u and dbar/ubar.
- MSTW2008 NNLO PDFs are disfavored by this data set

Data Sets for CT14

C T E Q

- There are a total of **2947** data points included from **33 experiments**, producing chi2=3252 at the best fit (with chi2/Npt=1.10).
- We can see from the values of chi2 that **the data and theory are in reasonable agreement for most experiments.**
- Values of the ``effective Gaussian variable'' Sn between -1 and +1 correspond to a good fit to the n-th experiment .

Large positive values correspond to a poor fit,

while large negative values are fit unusually well.

Data sets for CT14

CTEQ

TABLE I. Experimental data sets employed in the CT14 analysis. These are the lepton deep-inelastic scattering experiments. $N_{pt,n}$, χ_n^2 are the number of points and the value of χ^2 for the nth experiment at the global minimum. S_n is the effective Gaussian parameter [5,6,22] quantifying agreement with each experiment.

ID No.	Experimental data set		$N_{pt,n}$	χ_n^2	$\chi_n^2/N_{pt,n}$	S_n
101	BCDMS F_2^p	[23]	337	384	1.14	1.74
102	BCDMS F_2^d	[24]	250	294	1.18	1.89
104	NMC F_2^d/F_2^p	[25]	123	133	1.08	0.68
106	NMC σ_{red}^p	[25]	201	372	1.85	6.89
108	CDHSW F_2^p	[26]	85	72	0.85	−0.99
109	CDHSW F_3^p	[26]	96	80	0.83	−1.18
110	CCFR F_2^p	[27]	69	70	1.02	0.15
111	CCFR xF_3^p	[28]	86	31	0.36	−5.73
124	NuTeV $\nu\mu\mu$ semi-inclusive DIS	[29]	38	24	0.62	−1.83
125	NuTeV $\bar{\nu}\mu\mu$ semi-inclusive DIS	[29]	33	39	1.18	0.78
126	CCFR $\nu\mu\mu$ semi-inclusive DIS	[30]	40	29	0.72	−1.32
127	CCFR $\bar{\nu}\mu\mu$ semi-inclusive DIS	[30]	38	20	0.53	−2.46
145	H1 σ_r^b	[31]	10	6.8	0.68	−0.67
147	Combined HERA charm production	[32]	47	59	1.26	1.22
159	HERA1 combined DIS	[33]	579	591	1.02	0.37
169	H1 F_L	[34]	9	17	1.92	1.7

Data sets for CT14

C T E Q

TABLE II. The same as Table I, showing experimental data sets on Drell-Yan processes and inclusive jet production.

ID No.	Experimental data set		$N_{pt,n}$	χ^2_n	$\chi^2_n/N_{pt,n}$	S_n
201	E605 Drell-Yan process	[35]	119	116	0.98	−0.15
203	E866 Drell-Yan process, $\sigma_{pd}/(2\sigma_{pp})$	[36]	15	13	0.87	−0.25
204	E866 Drell-Yan process, $Q^3 d^2\sigma_{pp}/(dQdx_F)$	[37]	184	252	1.37	3.19
225	CDF run-1 electron A_{ch}, $p_{T\ell} > 25$ GeV	[38]	11	8.9	0.81	−0.32
227	CDF run-2 electron A_{ch}, $p_{T\ell} > 25$ GeV	[39]	11	14	1.24	0.67
234	D0 run-2 muon A_{ch}, $p_{T\ell} > 20$ GeV	[40]	9	8.3	0.92	−0.02
240	LHCb 7 TeV 35 pb^{-1} W/Z $d\sigma/dy_\ell$	[41]	14	9.9	0.71	−0.73
241	LHCb 7 TeV 35 pb^{-1} A_{ch}, $p_{T\ell} > 20$ GeV	[41]	5	5.3	1.06	0.30
260	D0 run-2 Z rapidity	[42]	28	17	0.59	−1.71
261	CDF run-2 Z rapidity	[43]	29	48	1.64	2.13
266	CMS 7 TeV 4.7 fb^{-1}, muon A_{ch}, $p_{T\ell} > 35$ GeV	[44]	11	12.1	1.10	0.37
267	CMS 7 TeV 840 pb^{-1}, electron A_{ch}, $p_{T\ell} > 35$ GeV	[45]	11	10.1	0.92	−0.06
268	ATLAS 7 TeV 35 pb^{-1} W/Z cross sec., A_{ch}	[46]	41	51	1.25	1.11
281	D0 run-2 9.7 fb^{-1} electron A_{ch}, $p_{T\ell} > 25$ GeV	[14]	13	35	2.67	3.11
504	CDF run-2 inclusive jet production	[47]	72	105	1.45	2.45
514	D0 run-2 inclusive jet production	[48]	110	120	1.09	0.67
535	ATLAS 7 TeV 35 pb^{-1} incl. jet production	[49]	90	50	0.55	−3.59
538	CMS 7 TeV 5 fb^{-1} incl. jet production	[50]	133	177	1.33	2.51

Theory Analysis in CT14

- CT14 contains 28 shape parameters, and CT10 has 25.
- CT14 has more flexible parametrizations – gluon, d/u at large x, both d/u and dbar/ubar at small x, and strangeness (assuming sbar = s) PDFs
- Non-perturbative parametrization form:

$$x\, f_a(x) = x^{a_1}\,(1-x)^{a_2}\, P_a(x)$$

where $P_a(x)$ is expressed as a linear combination of Bernstein polynomials to reduce the correlation among its coefficients.

- Produce 90% C.L. error PDF sets from Hessian method, scaled by 1/1.645 to obtain results at 68% C.L..

Theory Analysis in CT14

- When we perform global fit we choose exp. data with $Q^2 > 4$ GeV^2 and $W^2 > 12.5$ GeV^2 , namely, large-x data are not included to avoid large non-perturbative contributions.
- The PDFs for u, d, s (anti) quarks and the gluon are parametrized at an initial scale Q=1.3 GeV. PDFs at any other scale Q can be obtained from pQCD, via solving DGLAP evolution equations.
- Take $\alpha_s(Mz) = 0.118$ for NLO and NNLO; just like CT10 series, we also provide α_s-series PDFs.
- To deal with the heavy quark partons we use s-ACOT-χ prescription,
- In our global fit we have taken NNLO calculations for DIS, DY, W, Z cross sections, but for the jet cross sections we only use the NLO calculation but with NNLO PDF.
- Furthermore correlated systematic errors are taken into account when we do global fit.
- We also check our Hessian method results by Lagrange Multiplier method which does not assume quadratic approximation in chi-square calculations.

CT14 NNLO PDFs

Q= 2 GeV

Q= 100 GeV

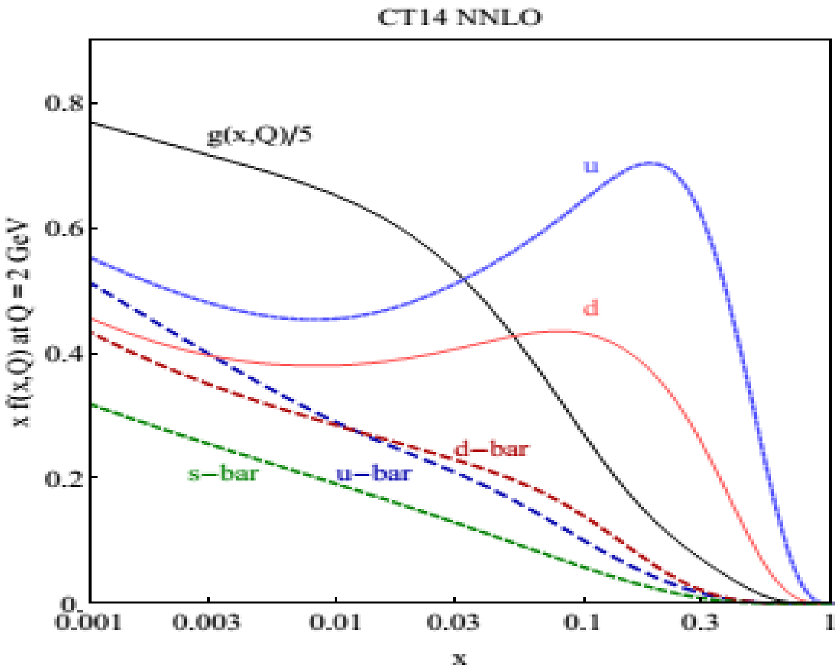

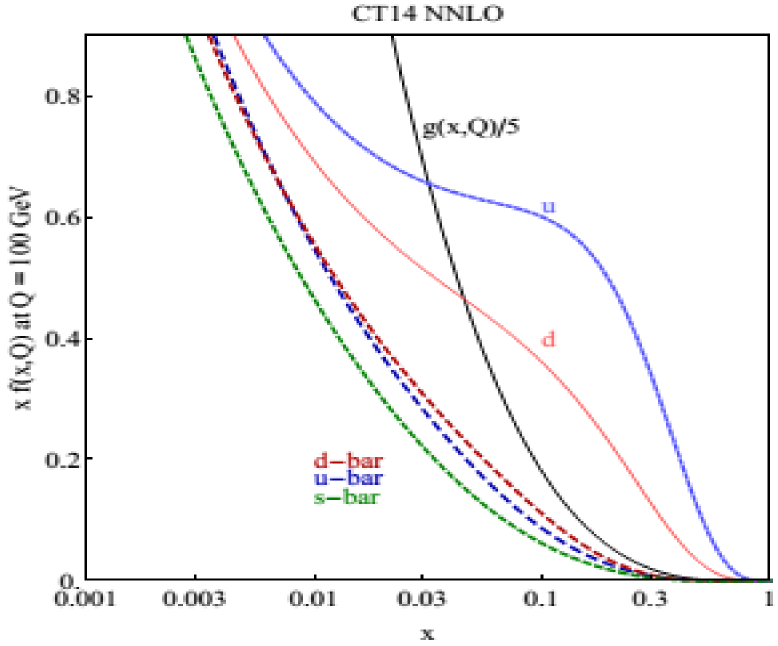

FIG. 4: The CT14 parton distribution functions at $Q = 2$ GeV and $Q = 100$ GeV for $u, \overline{u}, d, \overline{d}, s = \overline{s}$, and g.

Main features of CT10 are still present in CT14;

The antiquarks and quarks are comparable at low values of x and the antiquarks fall off in x even faster than the gluon

The u and d PDFs dominate at large values of x with u>d.

The gluon distribution dominates at low values of x and falls steeply as x increases .

CT14 NNLO PDFs

Typically CT14 NNLO PDFs have the following features:

- PDF error bands
  - u and d-quark PDFs are best known
  - In general there is really no constraint for x below 10E-4
  - large error for x above 0.3
  - Sea (e.g., ubar and dbar) quarks usually have larger uncertainties in large x region
  - Sea quarks are more non-perturbative parametrization form dependence in small x and large x regions
- PDF eigensets
  - useful for calculating PDF induced uncertainty
  - sensitive to some special combination of parton flavor(s).

CT14 vs. CT10 in u and ubar-PDFs

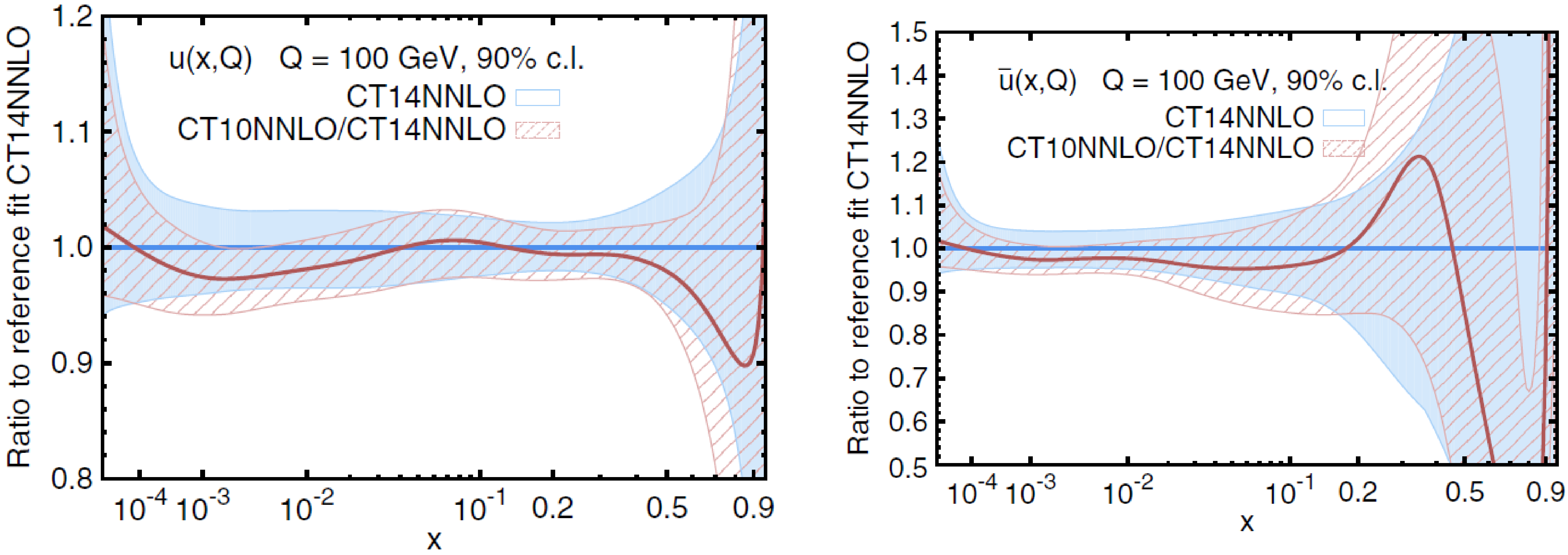

* $u(x,Q)$ and $\bar{u}(x,Q)$-PDFs are larger in CT14 than CT10 at $x < 10^{-2}$ due to flexible parametrization form.

* At $x = 0.2 - 0.5$ there are only very weak constraints on the sea quark PDFs, the new parametrization form of CT14 results in smaller values of $\bar{u}(x,Q)$ than CT10.

* At $x > 0.1$ the updated Tevatron D0 data has moderately increased u-quark PDFs.

CT14 vs. CT10 in d, dbar-PDFs

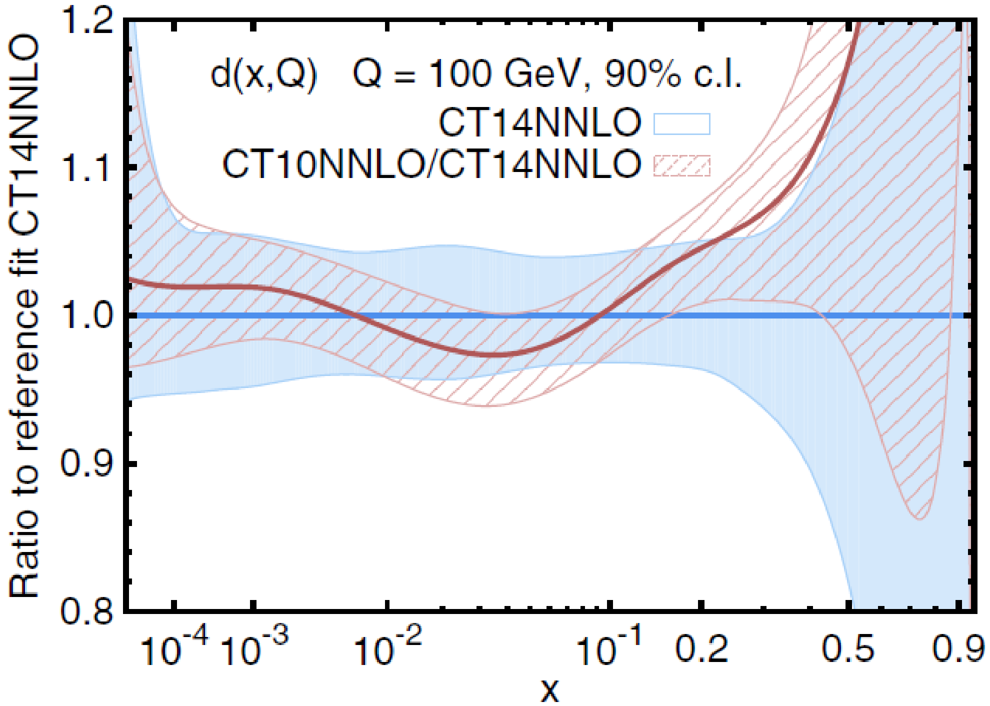

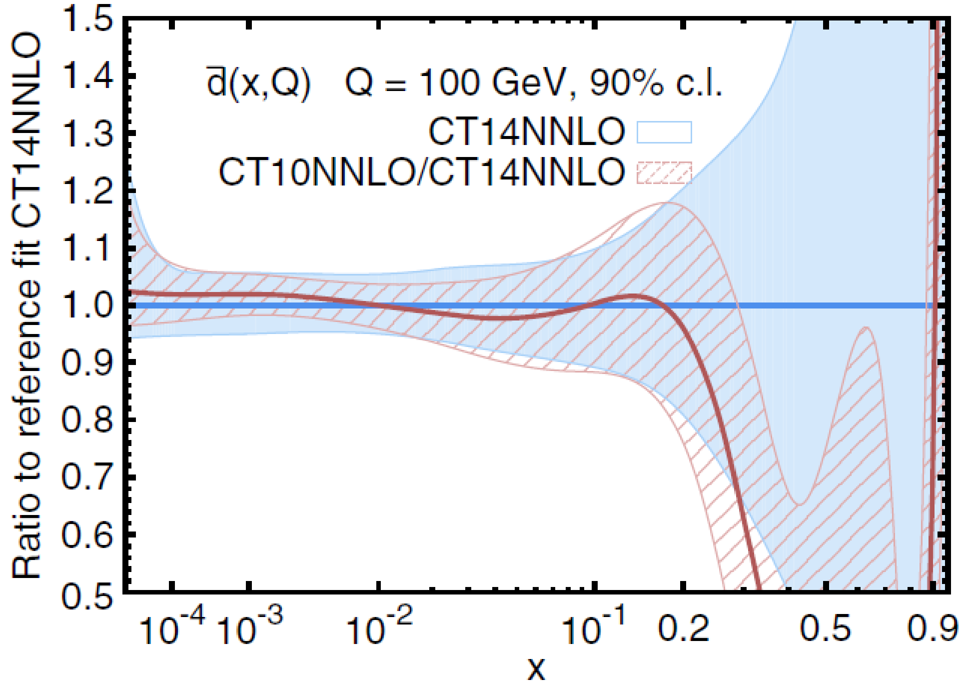

* The $d(x,Q)$ and $\bar{d}(x,Q)$-PDFs are smaller in CT14 than CT10 at $x < 10^{-2}$ due to more flexible parametrization form.

* The CT14 $d(x,Q)$-quark PDF has increased by 5% at $x = 0.05$ as a result of the inclusion of ATLAS and CMS W/Z production data at $7TeV$.

* At $x > 0.1$ the new Tevatron D0 data has reduced $d(x,Q)$-quark PDFs by large amount.

* $\bar{d}(x,Q)$-PDFs are larger in CT14 than CT10 at $x = 0.2 - 0.5$ due to new parametrization.

CT14 vs. CT10 in s-PDFs

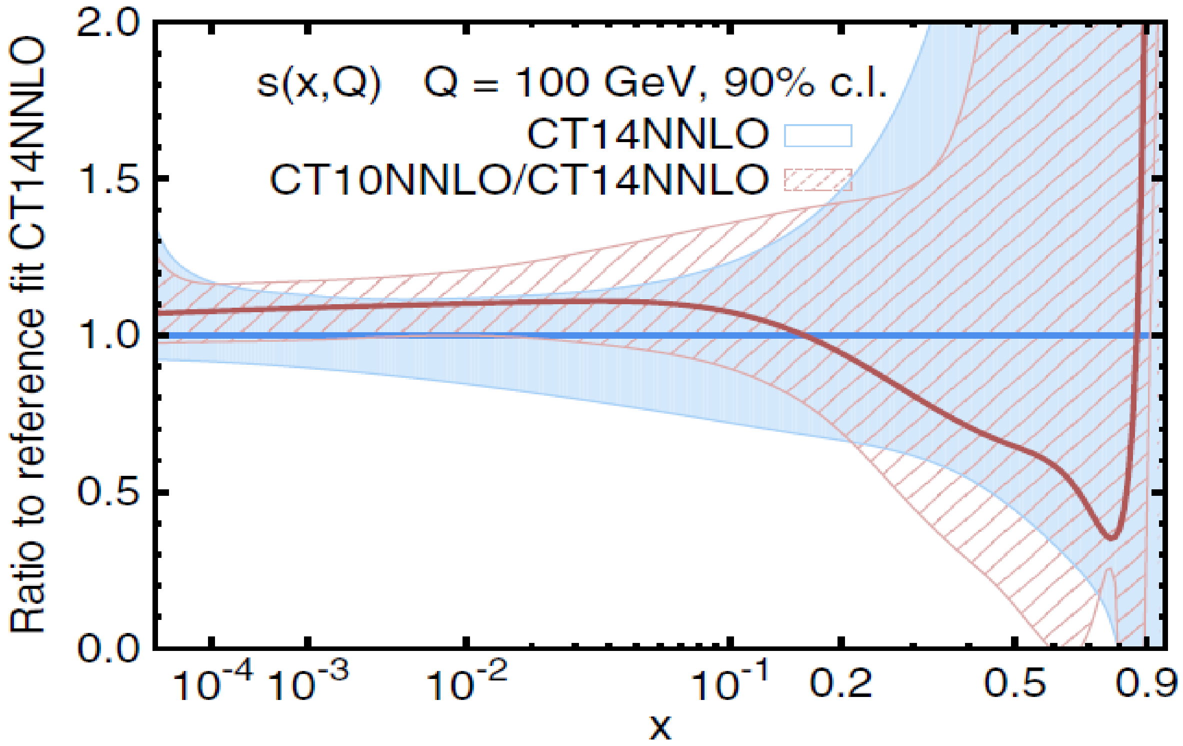

* The strangeness PDF $s(x, Q)$ has decreased for $0.01 < x < 0.15$, within the limits of the CT10 uncertainty, as a consequence of the more flexible parametrization, and the inclusion of the LHC data.
* The CT14 $s(x, Q)$ PDF is smaller than the CT10 for $x < 0.01$, because no data directly constraint it; its uncertainty remains large and compatible with that in CT10.
* At large x, above about 0.2, the strange quark PDF is essentially unconstrained in CT14, just as in CT10.

CT14 vs. CT10 in g-PDFs

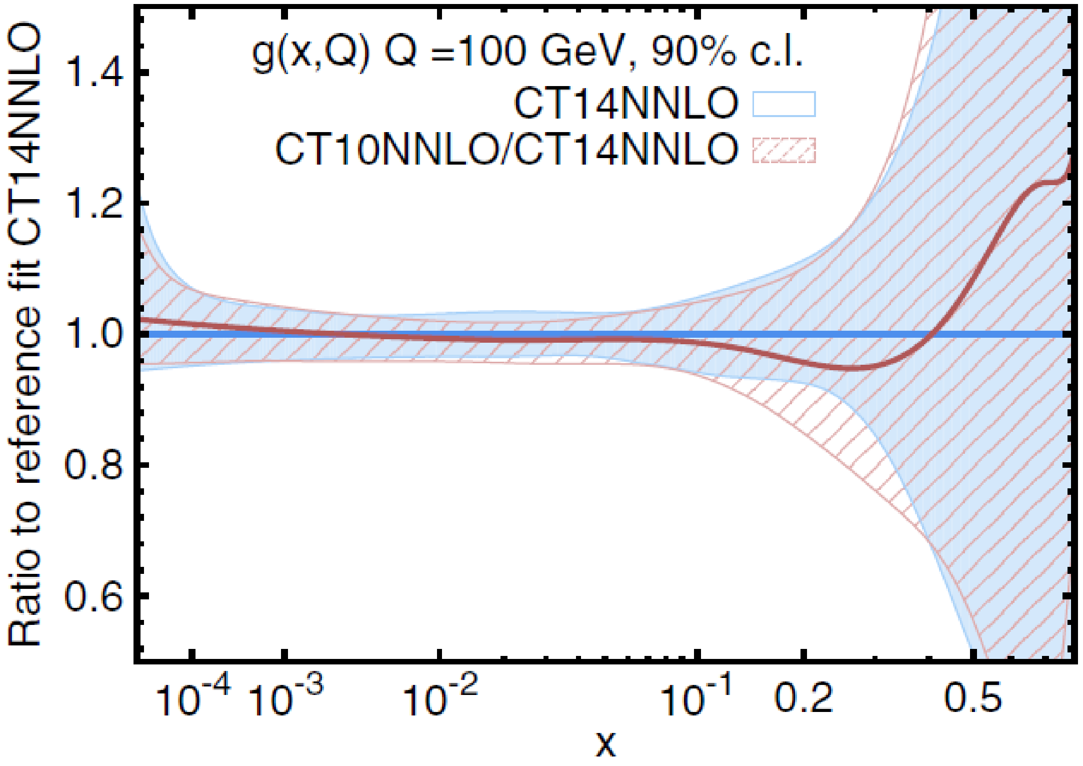

g-PDF is larger in CT14 than CT10 at x > 0.1 by the inclusion of the LHC jet data

CT14 vs. CT10 in d/u

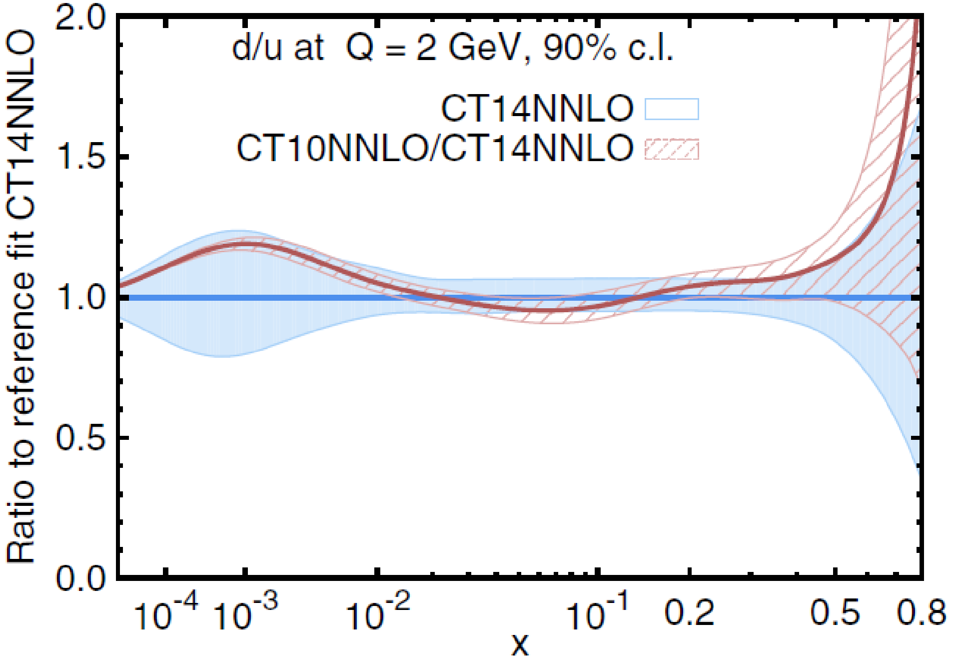

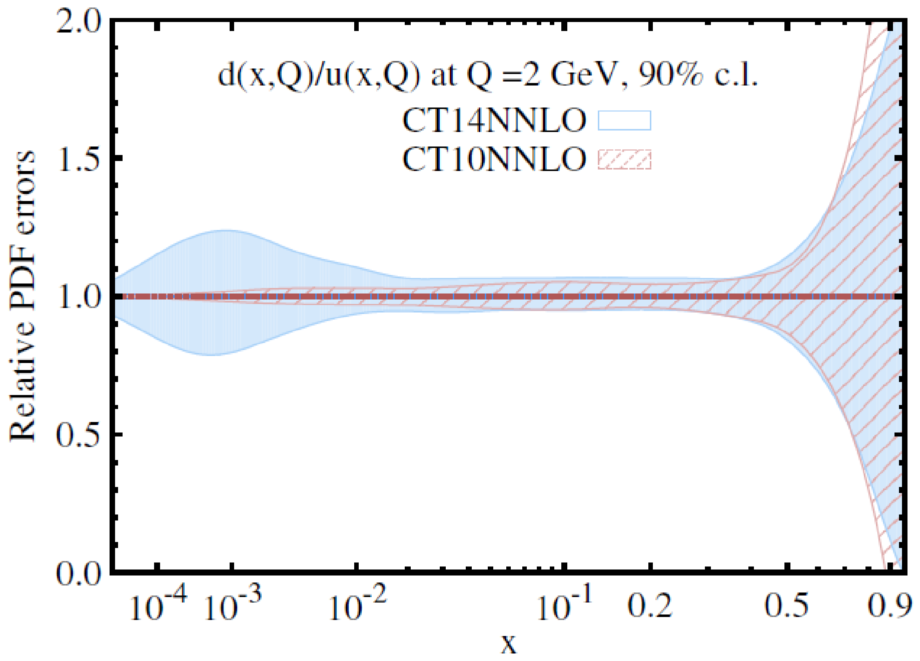

* d/u is smaller in CT14 than CT10 at $x > 0.1$ due to the $9.7 fb^{-1}$ D0 charge asym data.
* d/u uncertainty is larger in CT14 than CT10 $x < 0.05$ because of new parametrization form.
* At $x > 0.2$, the central CT14 NNLO ratio is lower than that of CT10 NNLO, while their relative PDF uncertainties remain about the same.

*Collider charge asymmetry data constrains d/u at x up to about 0.4. At even higher x, outside of the experimental reach, the behavior of the CT14 PDFs reflects the parametrization form, which now allows d/u to approach any constant value at $x \to 1$.

CT14 vs. CT10 in dbar/ubar

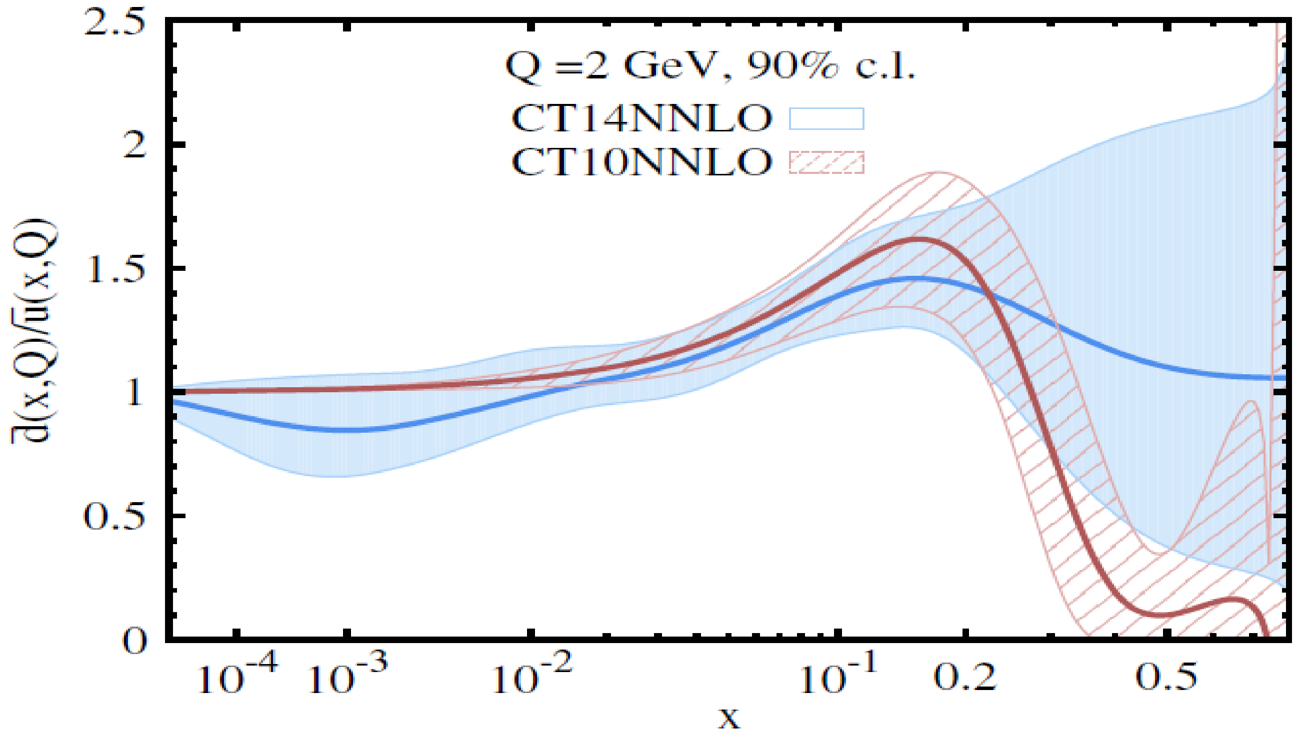

* The uncertainty on $\bar{d}/\bar{u}$ has increased across most of the x range .
* At $x > 0.1$, we assume that both $\bar{u}(x, Q_0)$ and $\bar{d}(x, Q_0)$ are proportional to $(1-x)^{a_2}$ with the same power a_2; the ratio $\bar{d}(x, Q_0)/\bar{u}(x, Q_0)$ can thus approach a constant value that comes out to be close to 1 in the central fit, while the parametrization forced it to vanish in CT10.

CT14 vs. CT10 in (s+sbar)/(ubar+dbar)

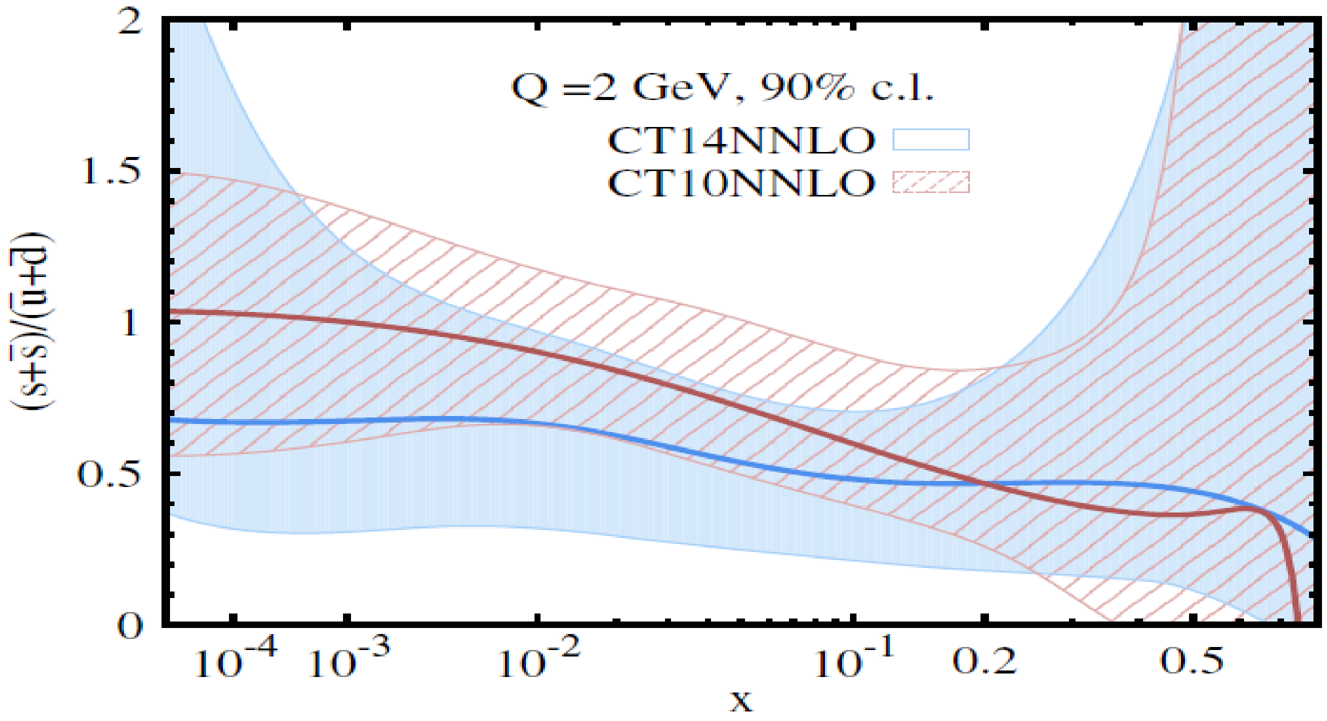

* The overall reduction in the strangeness PDF at $x > 0.01$ leads to a smaller ratio of the strange-to-nonstrange sea quark PDFs, $(s(x,Q) + \bar{s}(x,Q)) \,/\, (\bar{u}(x,Q) + \bar{d}(x,Q))$.

* At $x < 0.01$, this ratio is determined entirely by parametrization.

CT14 vs. CT10 in d/u

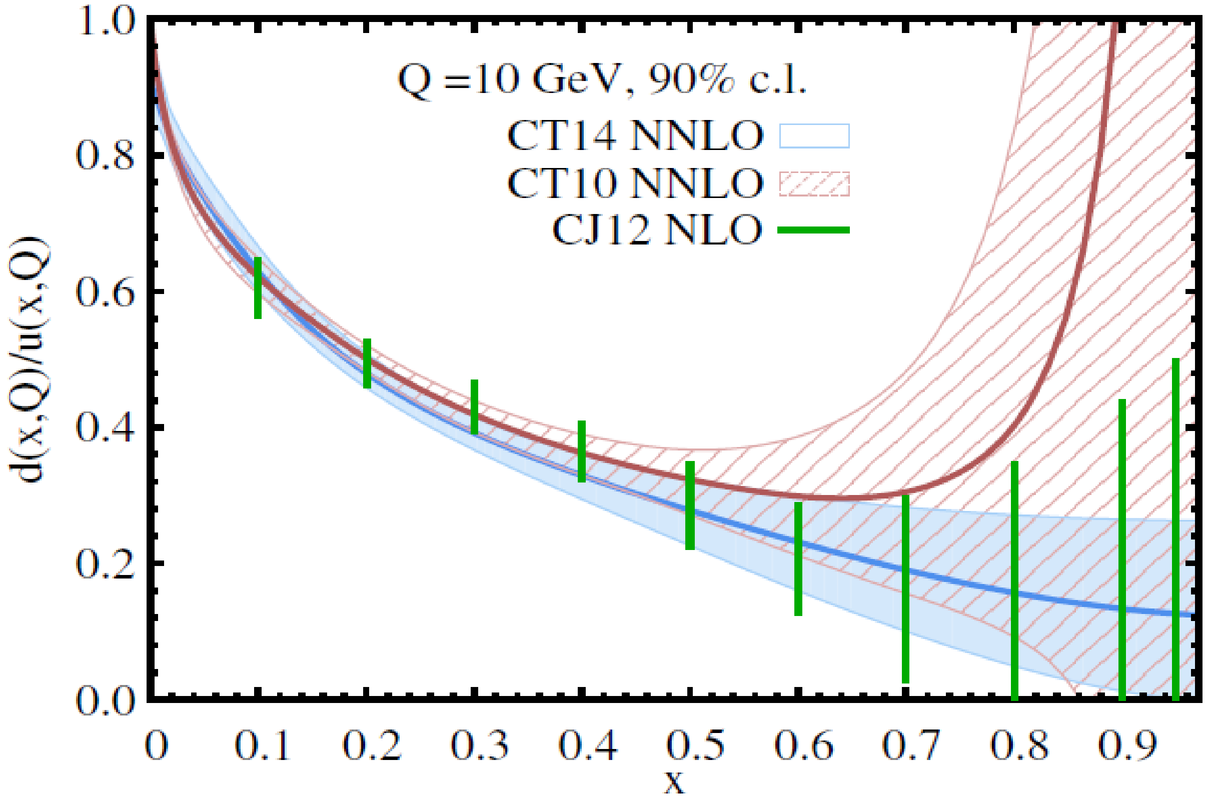

- In CT14, with more flexible parametrization and using Bernstein polynomial, assumes the ratio d/u approaches a constant as x -> 1
- CT14 agrees with CJ12 in large x region.

Checked by Lagrange Multiplier Method

- dbar/ubar at x around 0.2 and 0.3, mainly constrained by E866(pd/pp) data.
- dbar/ubar at x around 0.01, mainly constrained by NMC(F2d/F2p) data.
- d/u at x around 0.3, mainly constrained by NMC (F2d/F2p), E866 (pd/pp).
- Inclusion of LHC Run 1 W, Z and new Tevatron W data has impact on u, d, ubar and dbar PDFs.

Checked by Lagrange Multiplier Method

- The strangeness PDF s(x,Q) at x around 0.1, mainly constrained by NuTeV di-muon data.
- The strangeness PDF s(x,Q) at x around 0.01, mainly constrained by CCFR, NuTeV, di-muon data.
- Inclusion of LHCb W-lepton rapidity asymmetry data has impact on strangeness PDF s(x,Q) at small x.

Story about D0 Run 2 W-electron rapidity asymmetry data

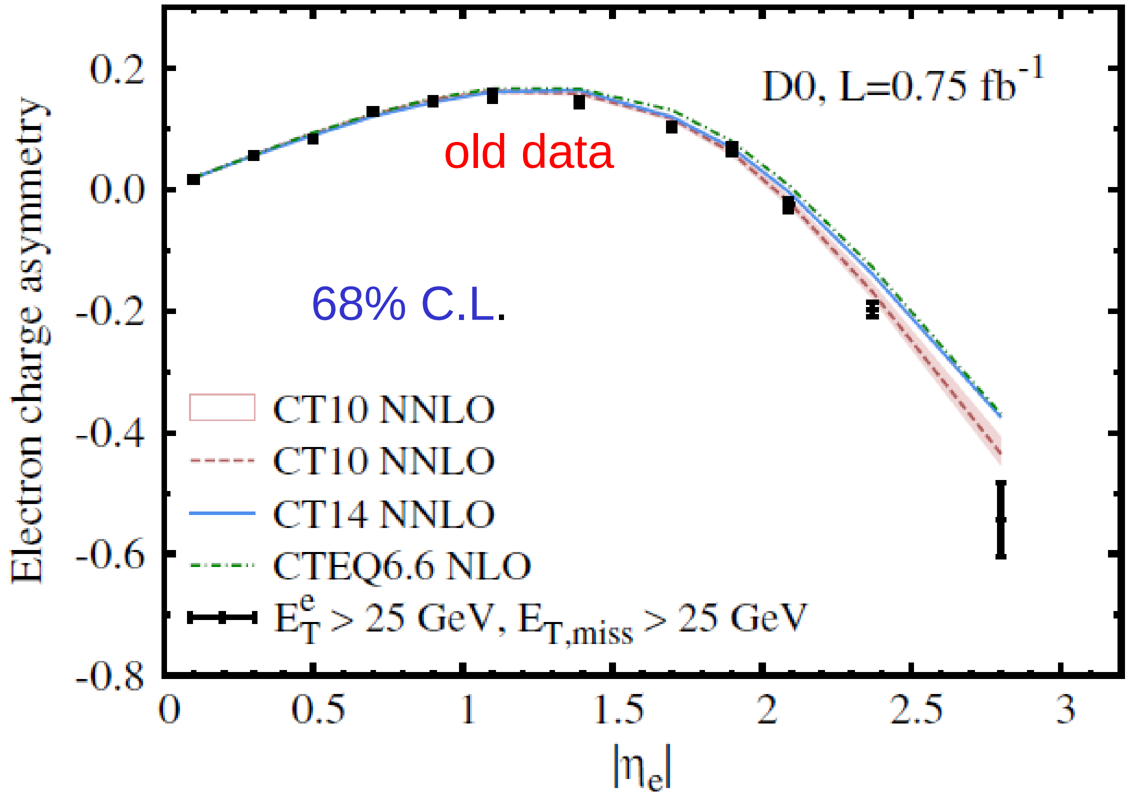

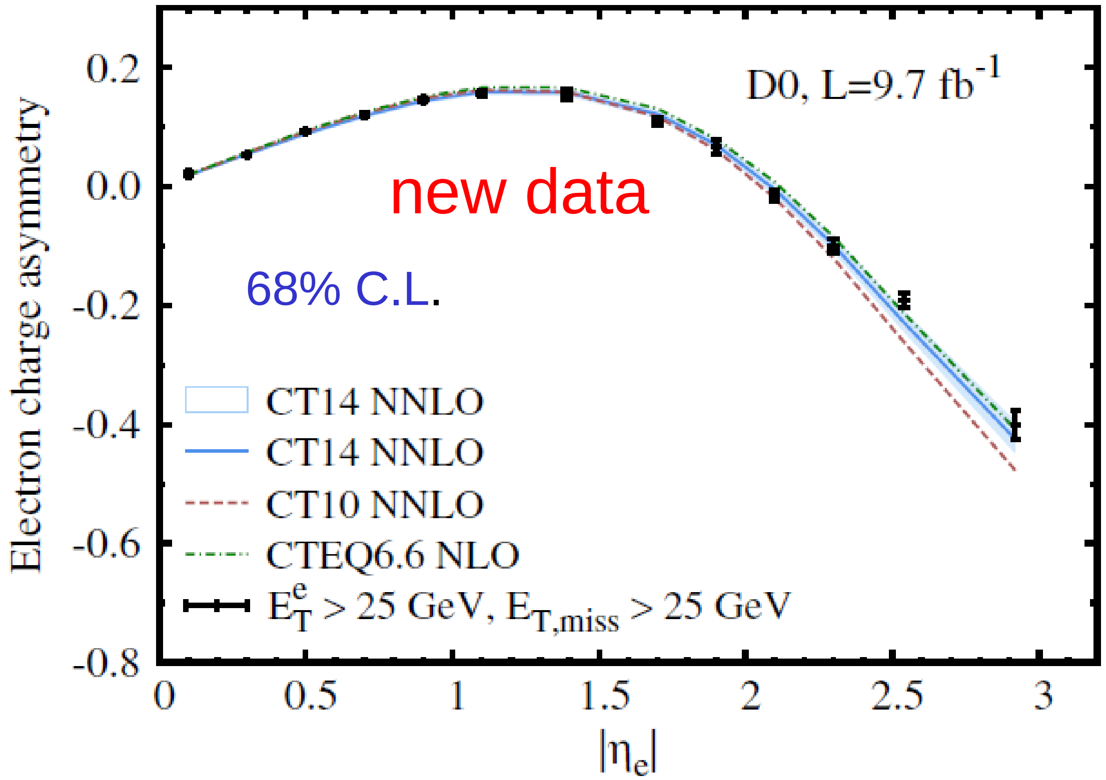

CT10 was produced by fitting to old D0 data.
CT14 uses new D0 data, closer to CTEQ6.6 than CT10 predictions in large rapidity.

Story about D0 Run 2 W-electron rapidity asymmetry data

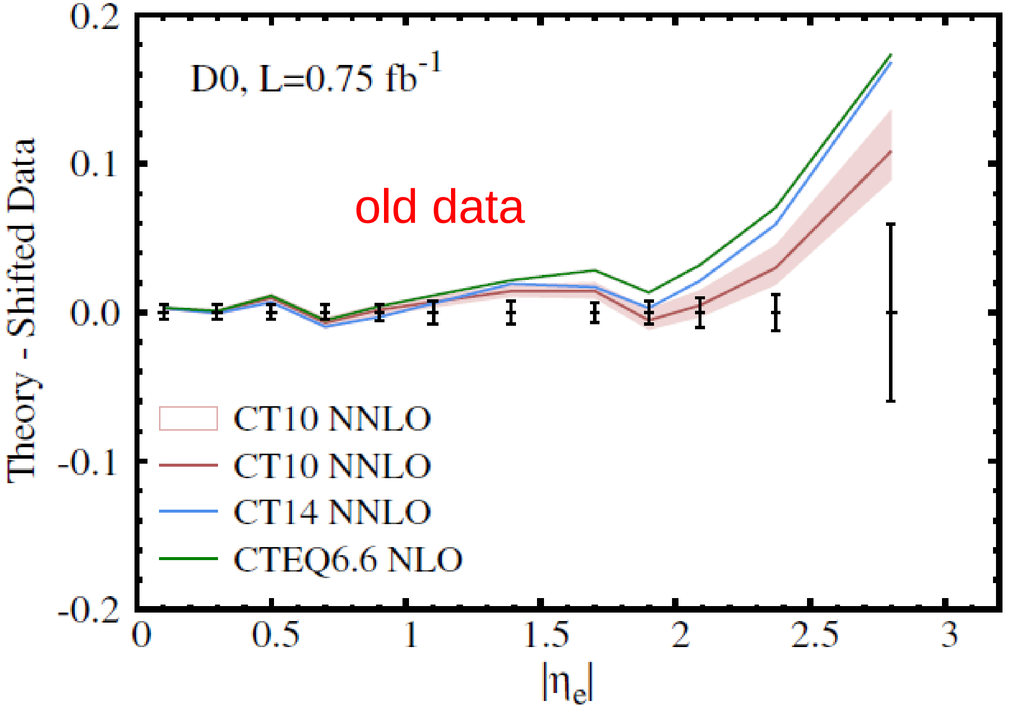

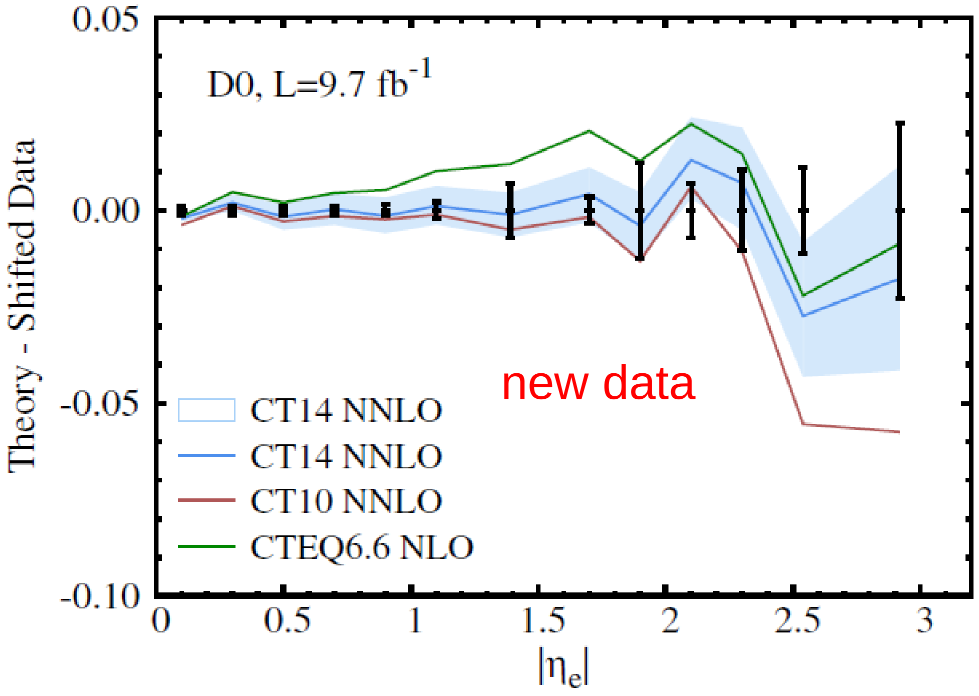

Old D0 data disfavor CTEQ6.6 and requires CT10.

New D0 data disfavor CT10 and requires CT14.

Correlation ellipse for W- vs. W+ inclusive cross sections

Vrap Code

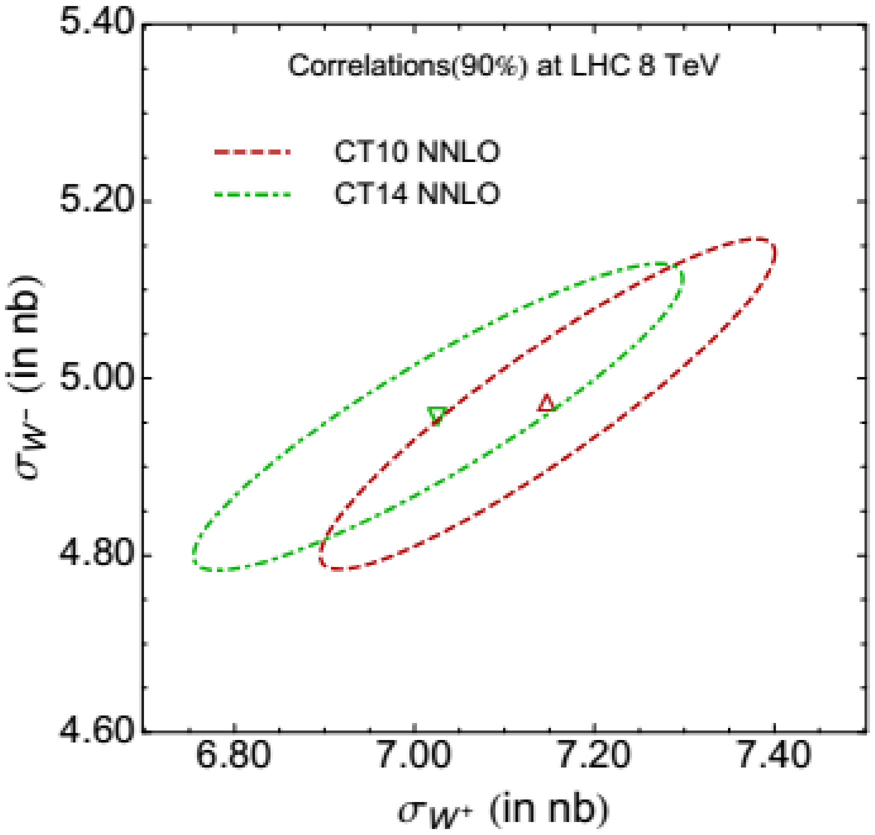

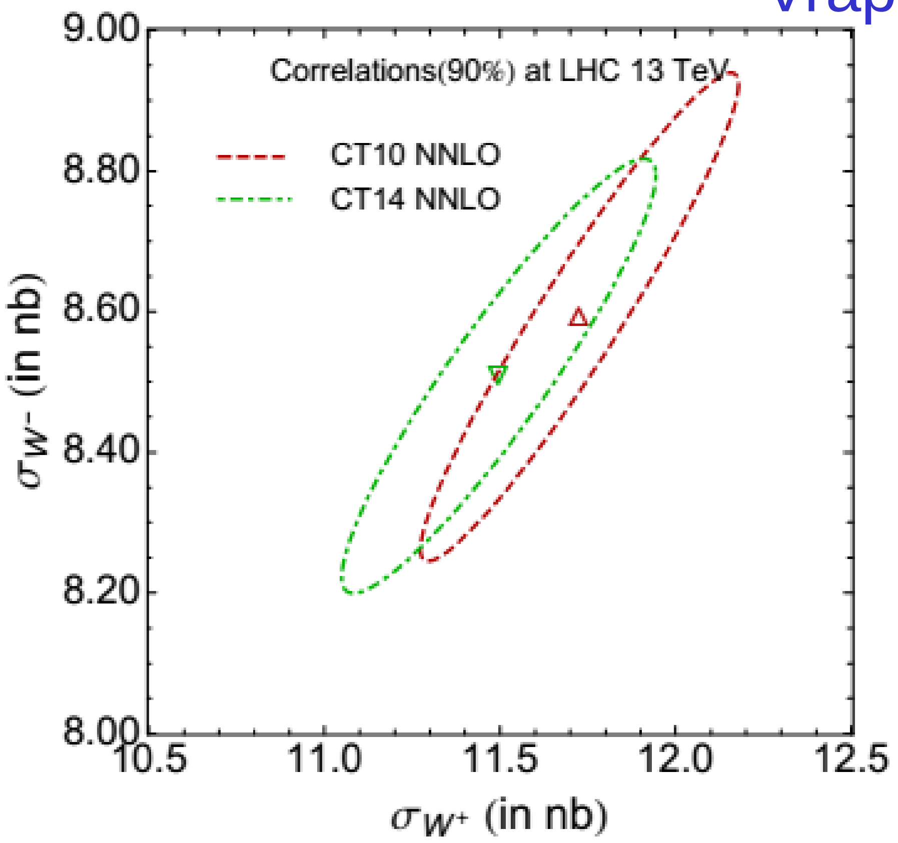

- CT14 and CT10 NNLO error ellipses for W − and W + cross sections at the LHC 8 and 13 TeV.
- W − and W + cross sections are highly correlated with each other.

W- and W+ cross sections decreases from CT10 to CT14.

Z vs. W

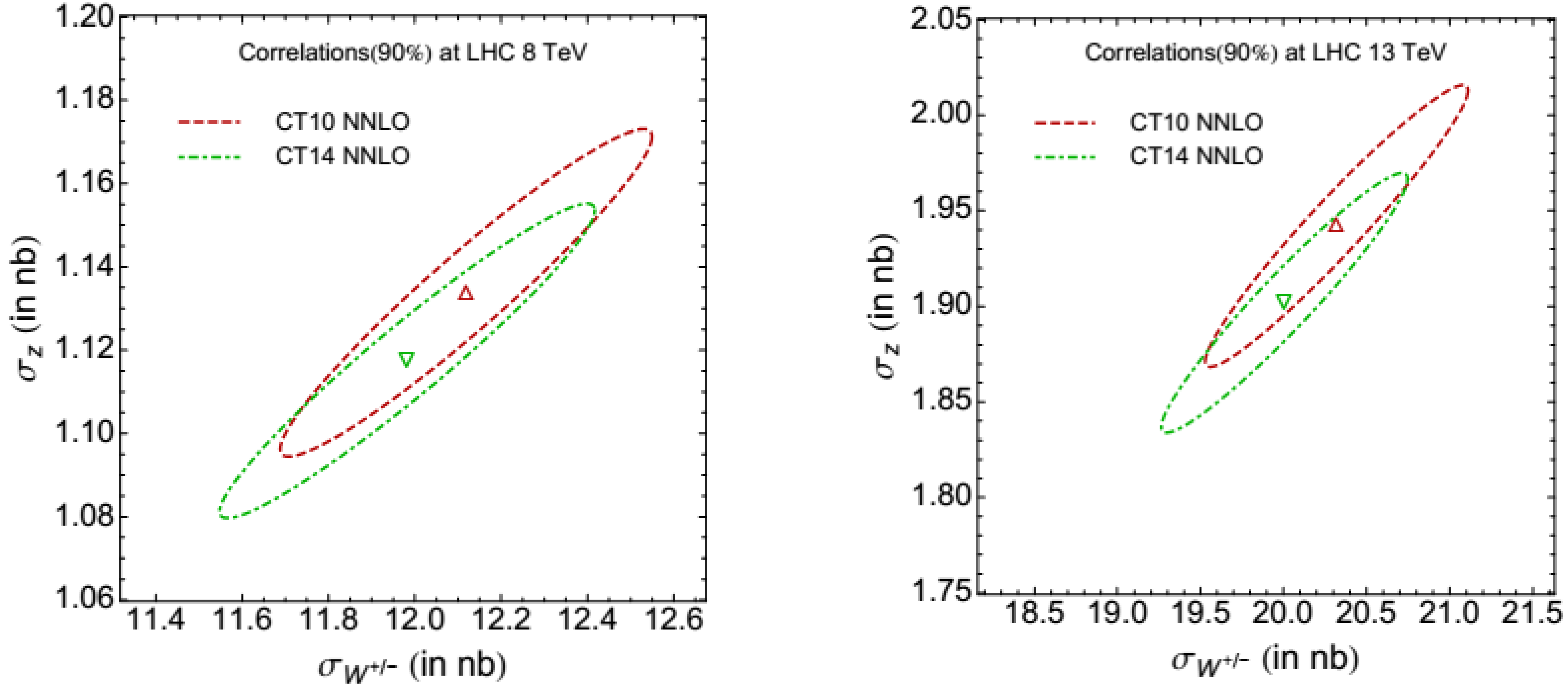

- W and Z cross sections are highly correlated with each other.
- W and Z cross sections decrease from CT10 to CT14.

t-tbar vs. Z

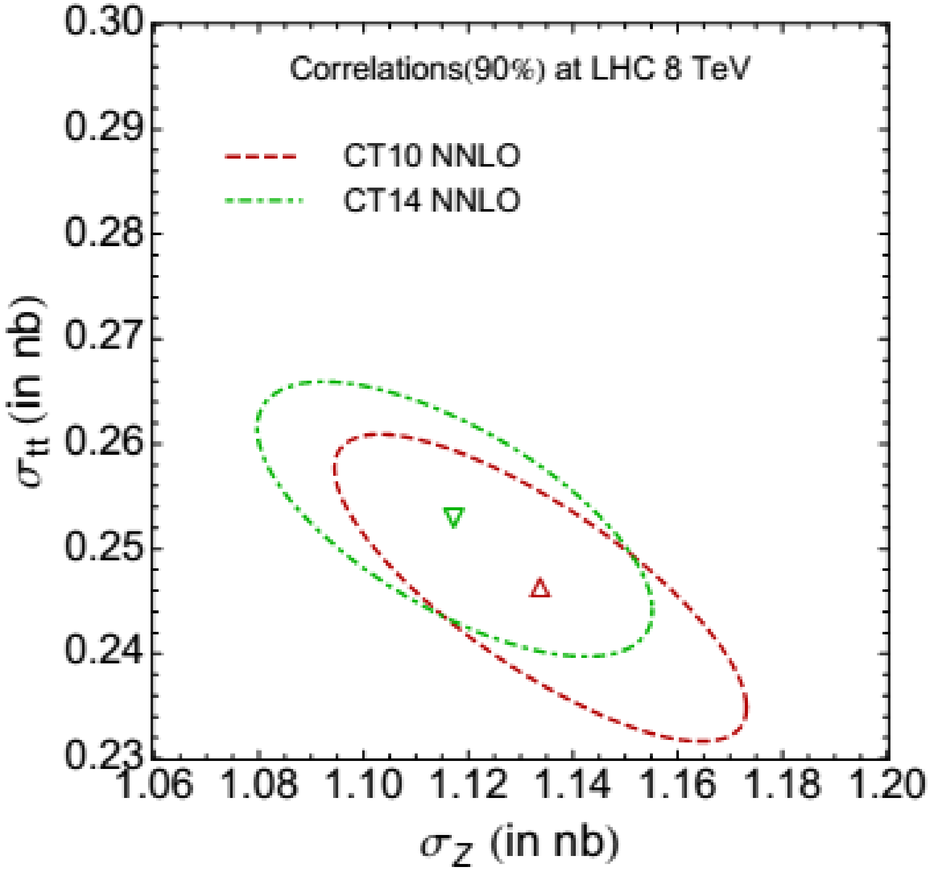

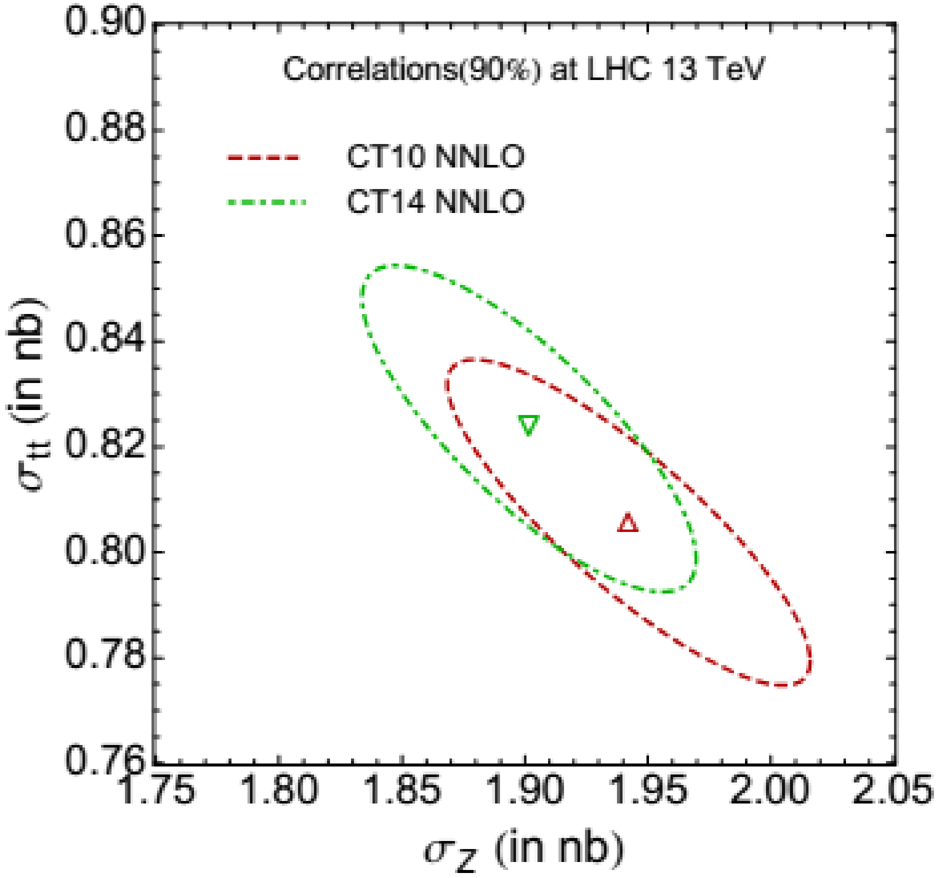

- t-tbar and Z boson production cross sections are anti correlated with each other.
- t-tbar cross section increase from CT10 to CT14.
- Z cross section decrease from CT10 to CT14.

t-tbar vs. ggH

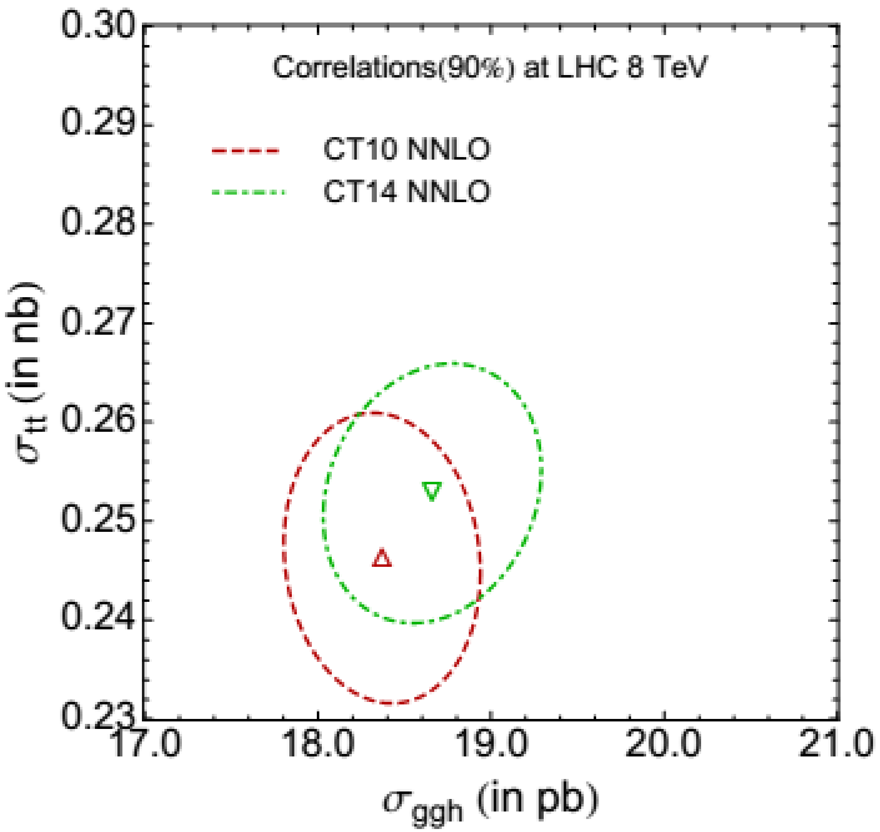

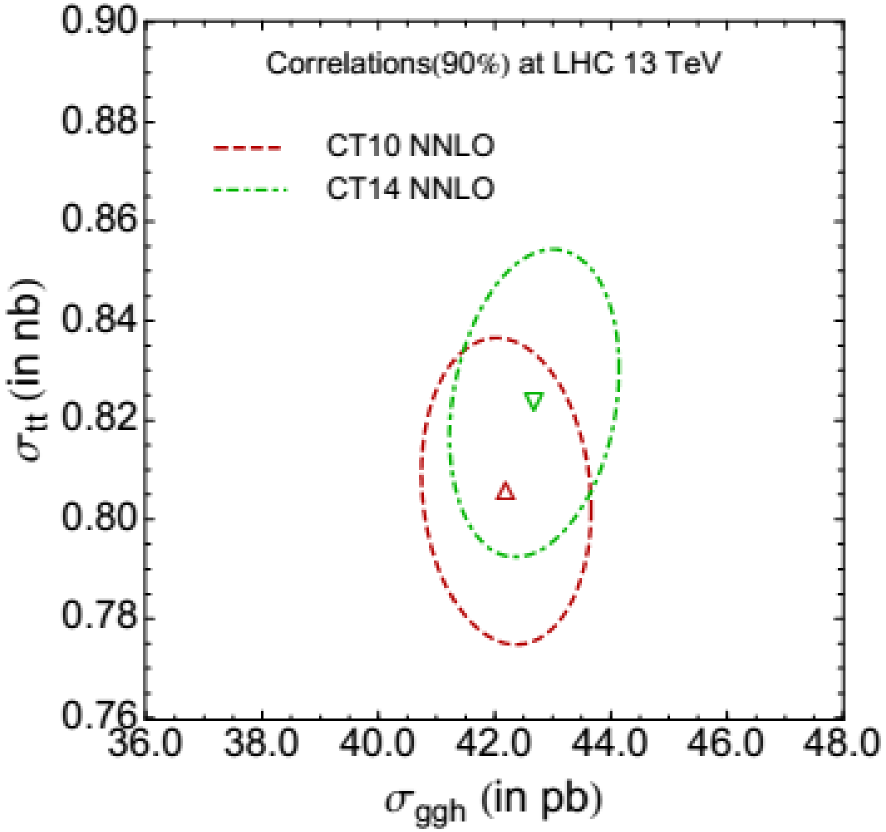

- t-tbar and ggH cross sections are correlated with each other
- t-tbar and ggH cross sections increase from CT10 to CT14, with slightly increase in correlation.

A comparison of ggH at NNLO

	CT14	MMHT2014	NNPDF3.0	CT10
8 TeV	$18.66^{+2.1\%}_{-2.3\%}$	$18.65^{+1.4\%}_{-1.9\%}$	$18.77^{+1.8\%}_{-1.8\%}$	$18.37^{+1.7\%}_{-2.1\%}$
13 TeV	$42.68^{+2.0\%}_{-2.4\%}$	$42.70^{+1.3\%}_{-1.8\%}$	$42.97^{+1.9\%}_{-1.9\%}$	$42.20^{+1.9\%}_{-2.5\%}$

- CT14 has perfect agreement in central value with MMHT and NNPDF.

t-tbar cross section

TABLE V. CT14 NNLO total inclusive cross sections for top-quark pair production at LHC center-of-mass energies of 7, 8, and 13 TeV.

$pp \to t\bar{t}$ (pb), PDF unc., $\alpha_s = 0.118$	7 TeV	8 TeV	13 TeV
68% C.L. (Hessian)	$177 + 4.4\% - 3.7\%$	$253 + 3.9\% - 3.5\%$	$823 + 2.6\% - 2.7\%$
68% C.L. (LM)		$+4.8\% - 4.6\%$	$+2.9\% - 2.9\%$
$pp \to t\bar{t}$ (pb), PDF $+ \alpha_s$	7 TeV	8 TeV	13 TeV
68% C.L. (Hessian)	$+5.5\% - 4.6\%$	$+5.2\% - 4.4\%$	$+3.6\% - 3.5\%$
68% C.L. (LM)		$+5.1\% - 4.7\%$	$+3.6\% - 3.5\%$

PDF luminosities

$$\sigma = \int dx_1 dx_2 \; g(x_1, M) g(x_2, M) \hat{\sigma}(M)$$

$$= \int d\tau dy \; g(x_1, M) g(x_2, M) \hat{\sigma}(M)$$

$$\equiv \int dM^2 \frac{dL}{dM^2} \hat{\sigma}(M)$$

PDF Luminosity

$$\tau = x_1 x_2$$

$$y = \frac{1}{2} \ln\left(\frac{x_1}{x_2}\right)$$

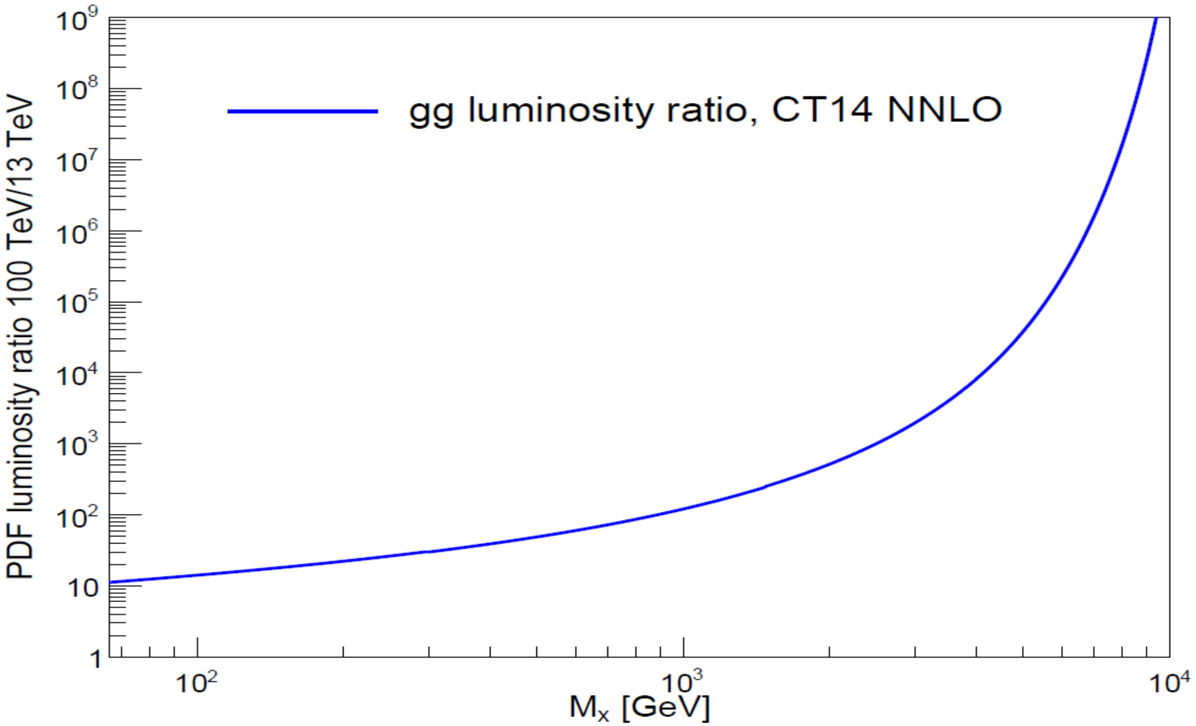

PDF luminosities are useful to translate differences in PDFs into differences in cross sections.

$M_X = Q$

Compare gluon-gluon parton luminosity

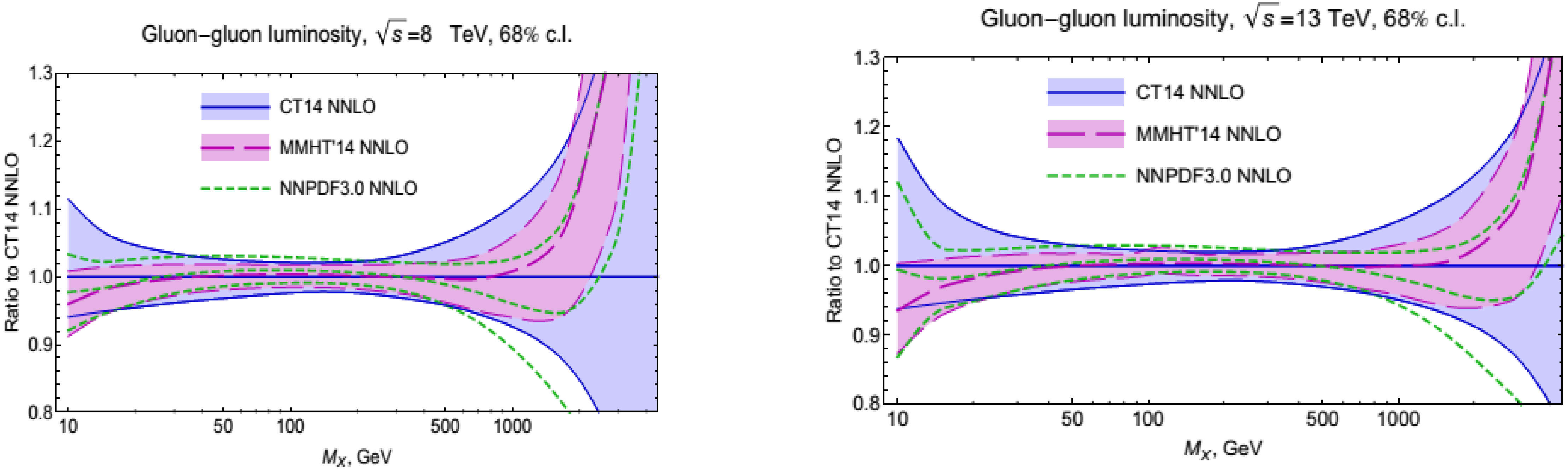

FIG. 33: The gg PDF luminosities for CT14, MMHT2014 [118] and NNPDF3.0 [83] at the LHC with $\sqrt{s} = 8$ and 13 TeV, with $\alpha_s = 0.118$.

Both the central values for the gg luminosity and the uncertainty bands agree very well among the 3 global PDFs, in the x range sensitive to Higgs production.

Summary

- CT14 has more flexible parametrization form and makes a different assumption about the behavior of d/u as x near 1, and dbar/ubar as x approaches to 0.
- CT14 is different from CT10, after including the LHC Run 1 (ATLAS, CMS, LHCb) W, Z and jet data and the new Tevatron D0 W-electron asymmetry data.
- We have checked that CT14 PDF error band is smaller than error bar of the published LHC Run 1data (such as high and low mass Drell-Yan) not included in our fit.
- CT14, at NNLO, NLO and LO, have been released.

  http://hep.pa.msu.edu/cteq/public/ct14.html
- Additional CT14 PDF sets (such as intrinsic charm, etc.) will also be released soon.

Some basics about PDFs

- Parton Distribution Function $f(x, \mathrm{Q})$
- Given a heavy resonance with mass Q produced at hadron collider with c.m. energy $\sqrt{S}$
- What's the typical x value?

$$< x >= \frac{Q}{\sqrt{S}}$$ at central rapidity (y=0)

- Generally, $x_1 = \frac{Q}{\sqrt{S}} e^{y}$ *and* $x_2 = \frac{Q}{\sqrt{S}} e^{-y}$

$$x_1 + x_2 = 2\frac{Q}{\sqrt{S}}\cosh(y) \Longrightarrow y_{\max}: \; x_1 + x_2 = 1$$

Experimental access to the proton structure

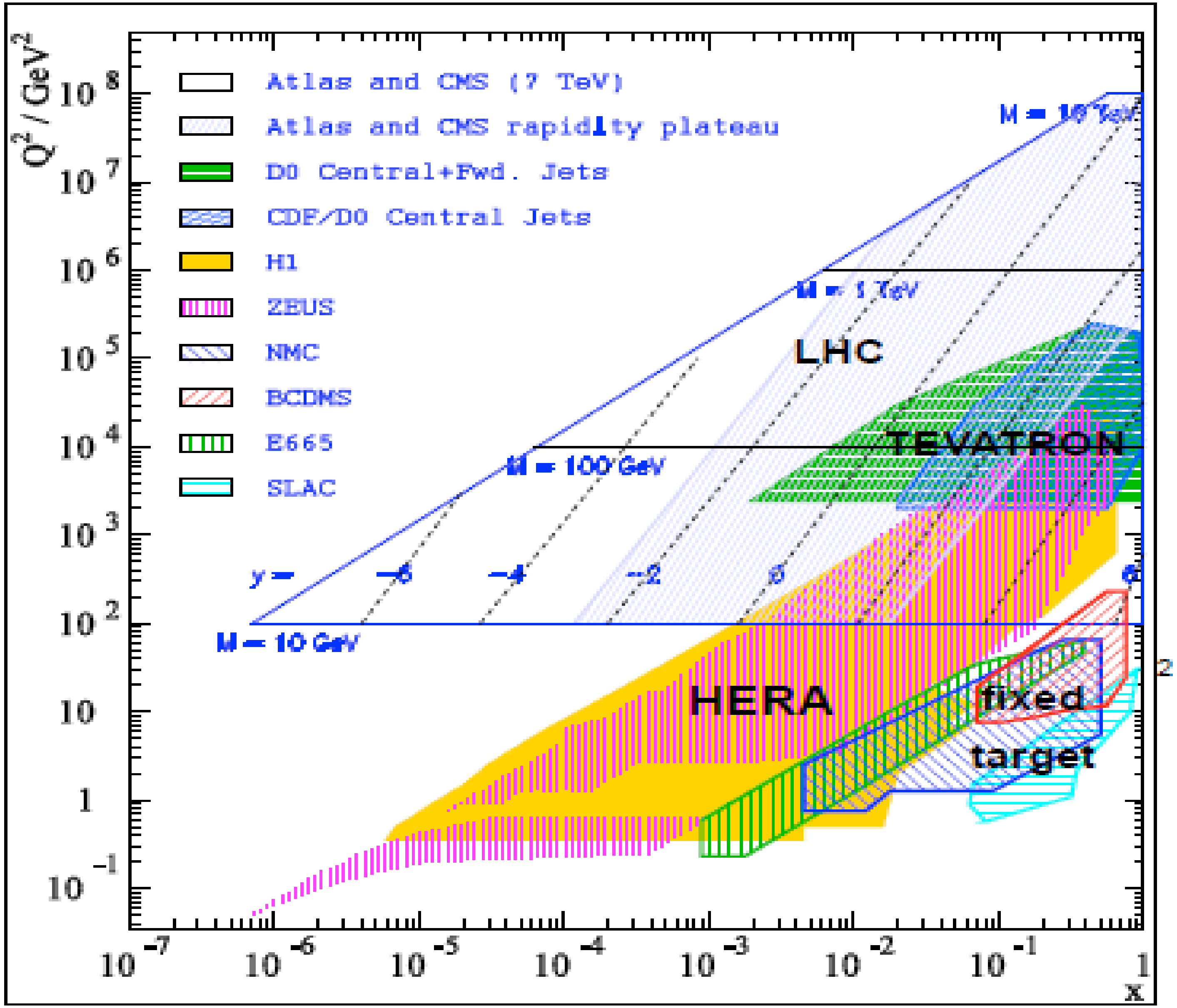

HERA: low and medium x

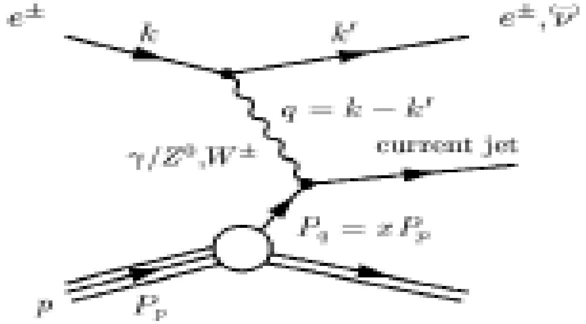

LHC: important constraints on g(x), flavour separation

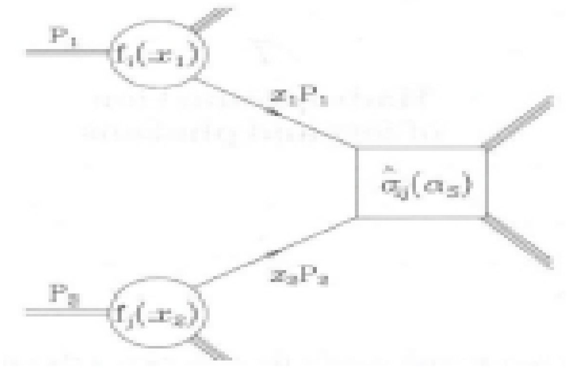

Fixed Target: high x, nuclear PDFs

On to a 100 TeV SppC

C T E Q

will access smaller x, larger Q^2

currently have no constraints on PDFs for x values below 1E-4

we don't know where at low x, BFKL effects start to become important

poor constraints (still) as well for high x PDFs

at high masses (Q^2), rely on DLAP evolution; we know at large Q^2, EW effects also become important

Kinematics of a 100 TeV FCC